https://doi.org/10.1093/plcell/koac139 THE PLANT CELL 2022: 34: 3066–3087

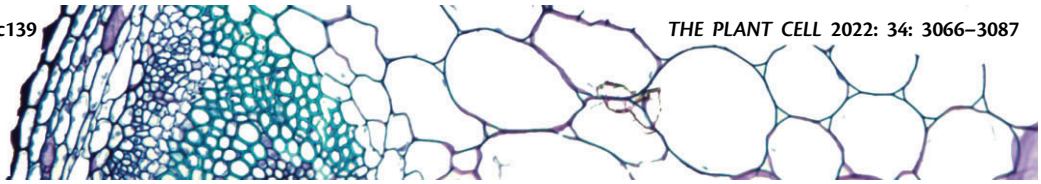

Research Article

Multilayered synergistic regulation of phytoalexin biosynthesis by ethylene, jasmonate, and MAPK signaling pathways in Arabidopsis

Jinggeng Zhou [1], Qiao Mu [1], Xiaoyang Wang [1], Jun Zhang [1], Haoze Yu [1], Tengzhou Huang [1], Yunxia He [1], Shaojun Dai [1] and Xiangzong Meng [1,*]

1 Shanghai Key Laboratory of Plant Molecular Sciences, College of Life Sciences, Shanghai Normal University, Shanghai 200234, China

*Author for correspondence: xzmeng@shnu.edu.cn

J.Zho. and X.M. designed the experiments. J.Zho., Q.M., X.W., J.Zha., H.Y., T.H., and Y.H. performed the experiments and analyzed the data. S.D. contributed new analytical tools. X.M. and J.Zho. wrote the article.

The author responsible for distribution of materials integral to the findings presented in this article in accordance with the policy described in the Instructions for Authors (https://academic.oup.com/plcell) is: Xiangzong Meng (xzmeng@shnu.edu.cn).

Abstract

Camalexin, an indolic antimicrobial metabolite, is the major phytoalexin in *Arabidopsis thaliana*, and plays a crucial role in pathogen resistance. Our previous studies revealed that the Arabidopsis mitogen-activated protein kinases MPK3 and MPK6 positively regulate pathogen-induced camalexin biosynthesis via phosphoactivating the transcription factor WRKY33. Here, we report that the ethylene and jasmonate (JA) pathways act synergistically with the MPK3/MPK6–WRKY33 module at multiple levels to induce camalexin biosynthesis in Arabidopsis upon pathogen infection. The ETHYLENE RESPONSE FACTOR1 (ERF1) transcription factor integrates the ethylene and JA pathways to induce camalexin biosynthesis via directly upregulating camalexin biosynthetic genes. ERF1 also interacts with and depends on WRKY33 to upregulate camalexin biosynthetic genes, indicating that ERF1 and WRKY33 form transcriptional complexes to cooperatively activate camalexin biosynthetic genes, thereby mediating the synergy of ethylene/JA and MPK3/MPK6 signaling pathways to induce camalexin biosynthesis. Moreover, as an integrator of the ethylene and JA pathways, ERF1 also acts as a substrate of MPK3/MPK6, which phosphorylate ERF1 to increase its transactivation activity and therefore further cooperate with the ethylene/JA pathways to induce camalexin biosynthesis. Taken together, our data reveal the multilayered synergistic regulation of camalexin biosynthesis by ethylene, JA, and MPK3/MPK6 signaling pathways via ERF1 and WRKY33 transcription factors in Arabidopsis.

Introduction

Plants have developed a multilayered immune system to recognize invading pathogens and mount efficient defense responses. Upon recognition of pathogen-associated molecular patterns (PAMPs) or pathogen-derived effectors, plants initiate early immune signaling events including the production of reactive oxygen species, activation of mitogen-activated protein kinases (MAPKs), and calcium-dependent protein kinases (CDPKs), and induction of defense hormones ethylene, jasmonic acid (JA), and salicylic acid (Jones and Dangl, 2006; Bigeard et al., 2015; Cui et al., 2015; Burger and Chory, 2019; Wang et al., 2020; Zhou and Zhang, 2020; DeFalco and Zipfel, 2021; Yuan et al., 2021). These early immune signals are then transduced to induce late-stage defense responses such as

Received August 30, 2021. Accepted May 03, 2022. Advance access publication May 11, 2022

defense gene activation, cell wall strengthening, and phytoalexin induction, to confer plant disease resistance (Meng and Zhang, 2013; Seybold et al., 2014; Qi et al., 2017; Burger and Chory, 2019).

Phytoalexins are low-molecular weight antimicrobial metabolites that are induced in plants upon pathogen infection and play crucial roles in plant disease resistance (Piasecka et al., 2015). In *Arabidopsis thaliana*, camalexin (3-thiazol-2′-yl-indole) is the most prominent phytoalexin, which accumulates to high levels in response to a variety of pathogens and is exported to the extracellular space by the PLEIOTROPIC DRUG RESISTANCE12 (PDR12) and PENETRATION3 (PEN3)/PDR8 transporters to defend against pathogens (Tsuji et al., 1992; Thomma et al., 1999; Bednarek et al., 2009; Schlaeppi et al., 2010; Stotz et al., 2011; Hiruma et al., 2013; He et al., 2019). Arabidopsis mutants defective in camalexin biosynthesis or transport exhibit enhanced susceptibility to a number of fungal and oomycetic pathogens, highlighting the importance of camalexin in plant resistance to these pathogens (Glazebrook and Ausubel, 1994; Thomma et al., 1999; Bednarek et al., 2009; Schlaeppi et al., 2010; Stotz et al., 2011; Hiruma et al., 2013; He et al., 2019).

Camalexin is an indolic metabolite derived from tryptophan (Trp) metabolism (Piasecka et al., 2015). In Arabidopsis, the first step of camalexin biosynthesis is the conversion of Trp to indole-3-acetaldoxime (IAOx) by two homologous cytochrome P450 enzymes, CYP79B2 and CYP79B3 (Zhao et al., 2002). From IAOx, several branches of indolic metabolism diverge, leading to the formation of camalexin, indole glucosinolates (IGs), auxin (indole-3-acetic acid), and several other indolics (Zhao et al., 2002; Nafisi et al., 2007; Sonderby et al., 2010). In the camalexin biosynthetic pathway, IAOx is later converted to indole-3-acetonitrile (IAN) by the P450 enzyme CYP71A13 (Nafisi et al., 2007). Thereafter, IAN is conjugated with glutathione by the glutathione S-transferase (GST) GSTF6 to form GS-IAN (Su et al., 2011), which is further processed by γ-glutamyl peptidases GGP1 and GGP3 to generate Cys-IAN (Geu-Flores et al., 2011). Finally, camalexin is synthesized from Cys-IAN via a two-step reaction catalyzed by the multifunctional P450 enzyme CYP71B15/PHYTOALEXIN DEFICIENT3 (PAD3; Zhou et al., 1999; Schuhegger et al., 2006; Bottcher et al., 2009).

In Arabidopsis, camalexin biosynthetic genes, including *CYP71A13* and *PAD3*, are expressed at very low levels in the absence of environmental stress and are highly induced by pathogen infection to activate camalexin biosynthesis (Schuhegger et al., 2006; Nafisi et al., 2007). The transcription factor WRKY33 has been shown to act as a key positive regulator of pathogen-induced camalexin biosynthesis (Qiu et al., 2008; Mao et al., 2011). Camalexin induction is largely blocked in *wrky33* mutants after infection by the fungal pathogen *Botrytis cinerea* or the bacterial pathogen *Pseudomonas syringae* (Qiu et al., 2008; Mao et al., 2011). In vivo binding of WRKY33 to the promoters of *CYP71A13* and *PAD3* indicates that WRKY33 directly activates these camalexin biosynthetic genes (Qiu et al., 2008; Mao et al., 2011; Birkenbihl et al., 2017).

The MAPKs, MPK3 and MPK6, positively regulate camalexin biosynthesis through phosphorylating WRKY33 (Ren et al., 2008; Mao et al., 2011). Recently, we found that the CDPKs, CPK5 and CPK6, also act as positive regulators of camalexin biosynthesis via phosphorylation of WRKY33 (Zhou et al., 2020). Interestingly, the MPK3/MPK6-mediated phosphorylation of WRKY33 on its N-terminal Ser residues enhances the transactivation activity of WRKY33, whereas CPK5 and CPK6 phosphorylate the Thr-229 residue of WRKY33 to increase its DNA binding ability (Zhou et al., 2020). Therefore, MPK3/MPK6 and CPK5/CPK6 cooperatively regulate camalexin biosynthesis through differential phospho-regulation of WRKY33 activity.

Besides pathogen-responsive protein kinases, defense hormones induced by pathogen attack also play crucial roles in plant immunity (Burger and Chory, 2019; Aerts et al., 2021). In contrast to SA, which is involved in plant resistance to biotrophic and semibiotrophic pathogens (Peng et al., 2021), ethylene and JA act synergistically against necrotrophic pathogen infection (Burger and Chory, 2019). Once produced, ethylene binds to and inactivates its receptors, which consequently inhibits the protein kinase CTR1-mediated phosphorylation of ETHYLENE INSENSITIVE2 (EIN2), the central positive regulator of ethylene signaling (Ju and Chang, 2015; Binder, 2020). The C-terminus of the nonphosphorylated EIN2 is then cleaved and enters the nuclei, where it activates the transcription factors EIN3/EIN3-LIKE1 (EIL1) to mediate ethylene-responsive gene expression and defense responses (Ju and Chang, 2015; Binder, 2020).

In the JA signaling pathway, perception of JA by the F-box protein CORONATINE INSENSITIVE1 (COI1) promotes physical interaction between COI1 and JASMONATE-ZIM DOMAIN (JAZ) repressor proteins, thus leading to the degradation of JAZs and thereafter the derepression of JAZ-interacting transcription factors, such as EIN3/EIL1, to induce defense responses (Song et al., 2014; Zhang et al., 2017a; Howe et al., 2018). Downstream of EIN3/EIL1, the APETALA2/ETHYLENE RESPONSE FACTOR (AP2/ERF) family transcription factors, such as ERF1, OCTADECANOID-RESPONSIVE ARABIDOPSIS59 (ORA59) and ERF96, act directly to induce ethylene/JA-responsive genes, such as *PDF1.2* (Solano et al., 1998; Lorenzo et al., 2003; Pre et al., 2008; Catinot et al., 2015; Huang et al., 2016). Therefore, EIN3/EIL1 and ERF transcription factors function as integrators to mediate the synergy of ethylene and JA pathways in regulating defense gene expression (Lorenzo et al., 2003; Pre et al., 2008; Zhu et al., 2011; Huang et al., 2016). Ethylene and JA signaling pathways were also implicated in regulating camalexin biosynthesis (Thomma et al., 1999; Zhou et al., 1999; Zhang et al., 2017b), but the underlying mechanisms remain elusive.

In this study, we found that ethylene and JA pathways act through the ERF1 transcription factor to synergistically induce pathogen-responsive camalexin biosynthesis in

Arabidopsis. Moreover, MPK3/MPK6 was revealed to phosphoactivate ERF1 and therefore act synergistically with ethylene/JA pathways via ERF1 to induce camalexin biosynthesis. Furthermore, we showed that ERF1 and WRKY33 form transcriptional complexes to cooperatively activate camalexin biosynthetic genes, thereby further mediating the synergy of ethylene/JA and MPK3/MPK6 signaling pathways to induce camalexin biosynthesis. Collectively, our findings in this study reveal the multilayered synergistic regulation of camalexin biosynthesis by ethylene, JA, and MPK3/MPK6 signaling pathways via ERF1 and WRKY33 transcription factors in Arabidopsis upon infection by pathogens.

Results

Synergistic activation of camalexin biosynthesis by the ethylene and JA signaling pathways

Plant responses to pathogen attack include the activation of secondary metabolic reprogramming (Piasecka et al., 2015). To identify the potential antimicrobial metabolites induced by ethylene and JA pathways, we profiled the metabolites secreted into the liquid culture medium by Arabidopsis wild-type (Columbia-0 [Col-0]) seedlings after treatment with methyl jasmonate (MeJA) and/or the ethylene precursor 1-aminoaminocyclopropane-1-carboxylic acid (ACC), which can be rapidly converted to ethylene in plants.

High-performance liquid chromatography (HPLC) analyses with fluorescence detection revealed that a metabolite in the Col-0 seedling culture was induced by ACC/MeJA cotreatment but not by treatment of either ACC or MeJA (Supplemental Figure S1; Figure 1A), suggesting that this metabolite was synergistically induced by ethylene/JA pathways. This metabolite had the same retention time as the synthetic camalexin standard in HPLC analyses (Supplemental Figure S1), indicating that it is camalexin. The loss of this ACC/MeJA-induced metabolite in the culture medium of the camalexin-null mutant *pad3-1* confirmed that ethylene and JA pathways synergistically induce camalexin production in Arabidopsis (Figure 1B).

Consistent with the synergistic action of ACC and MeJA in camalexin induction, as shown in Figure 1C, the expression of camalexin biosynthetic genes *CYP71A13* and *PAD3* were highly induced by ACC/MeJA cotreatment but only mildly upregulated by either ACC or MeJA treatment, indicating that the ethylene and JA pathways synergistically activate camalexin biosynthetic genes, thereby inducing camalexin biosynthesis. Blocking either ethylene signaling in the *ein2-1* mutant or JA signaling in the *coi1-1* mutant completely abolished the ACC/MeJA-induced camalexin production (Figure 1D), indicating the coaction and interdependency of ethylene and JA signaling pathways in activating camalexin biosynthesis.

To further investigate the role of ethylene and JA pathways in pathogen-induced camalexin biosynthesis, we examined the camalexin induction in *ein2-1* and *coi1-1* mutants after infection by *B. cinerea*. As shown in Figure 1E, the *B. cinerea*-induced levels of camalexin production in *ein2-1* and *coi1-1* mutants were both reduced to ~60% of that in wild-type plants. Consistent with this, the induction of camalexin biosynthetic genes *CYP71A13* and *PAD3* by *B. cinerea* infection was also significantly compromised in both *ein2-1* and *coi1-1* mutants (Figure 1F).

To further reveal the relationship between ethylene and JA pathways in regulating pathogen-induced camalexin biosynthesis, we further generated the *ein2-1 coi1-1* double mutant. Figure 1E shows that the level of camalexin production in *ein2-1 coi1-1* induced by *B. cinerea* infection was comparable with that in either parental single mutant, that is, ~60% of that in wild-type plants. Consistent with this, the inductions of *CYP71A13* and *PAD3* expression in *ein2-1 coi1-1* were not further reduced compared with those in *ein2-1* and/or *coi1-1* (Figure 1F). Together, these data indicate that the ethylene and JA pathways act interdependently and synergistically to induce camalexin biosynthesis via activating camalexin biosynthetic genes in Arabidopsis upon *B. cinerea* infection.

The ERF1 transcription factor plays a crucial role in activating camalexin biosynthesis upon *B. cinerea* infection

Ethylene and JA signaling are often transduced and integrated through the AP2/ERF family transcription factors (Huang et al., 2016). Several ERFs, including ERF1, ORA59, and ERF96, have been shown to act downstream of the ethylene/JA pathways and integrate ethylene/JA signaling to directly regulate defense gene expression (Lorenzo et al., 2003; Pre et al., 2008; Catinot et al., 2015). Therefore, in search for the transcription factor(s) regulating camalexin biosynthesis downstream of ethylene/JA, we tested the involvement of ERF1, ORA59, and ERF96 in camalexin induction by *B. cinerea* infection. To this end, we generated two *erf1* mutants (*erf1-c1* and *erf1-c2*) using the clustered regularly interspaced short palindromic repeats (CRISPR)/CRISPR-associated protein 9 (Cas9) system (Supplemental Figure S2A), obtained the *ora59-1* T-DNA insertional mutant from the Arabidopsis Biological Resource Center (ABRC), and further generated the *ora59-1 erf96-c1* double mutant via CRISPR/Cas9 system (Supplemental Figure S2B). As shown in Figure 2A and Supplemental Figure S3, camalexin production induced by *B. cinerea* infection was significantly compromised in the *erf1-c1* and *erf1-c2* mutants but not in the *ora59-1* or *ora59-1 erf96-c1* mutant, indicating that ERF1 but not ORA59 or ERF96 positively regulates *B. cinerea*-induced camalexin biosynthesis. The compromised camalexin induction in *erf1-c1* mutant was correlated with the significantly attenuated activation of camalexin biosynthetic genes *CYP71A13* and *PAD3* after *B. cinerea* infection (Figure 2B).

We then further tested the effect of *ERF1* overexpression driven by the *35S* promoter on *B. cinerea*-responsive camalexin biosynthesis. Figure 2, A, B, and D show that overexpression of *ERF1* greatly potentiated the induction of camalexin biosynthesis and the activation of camalexin biosynthetic genes *CYP71A13* and *PAD3* in response to *B. cinerea* infection. Therefore, these data indicate that ERF1 acts

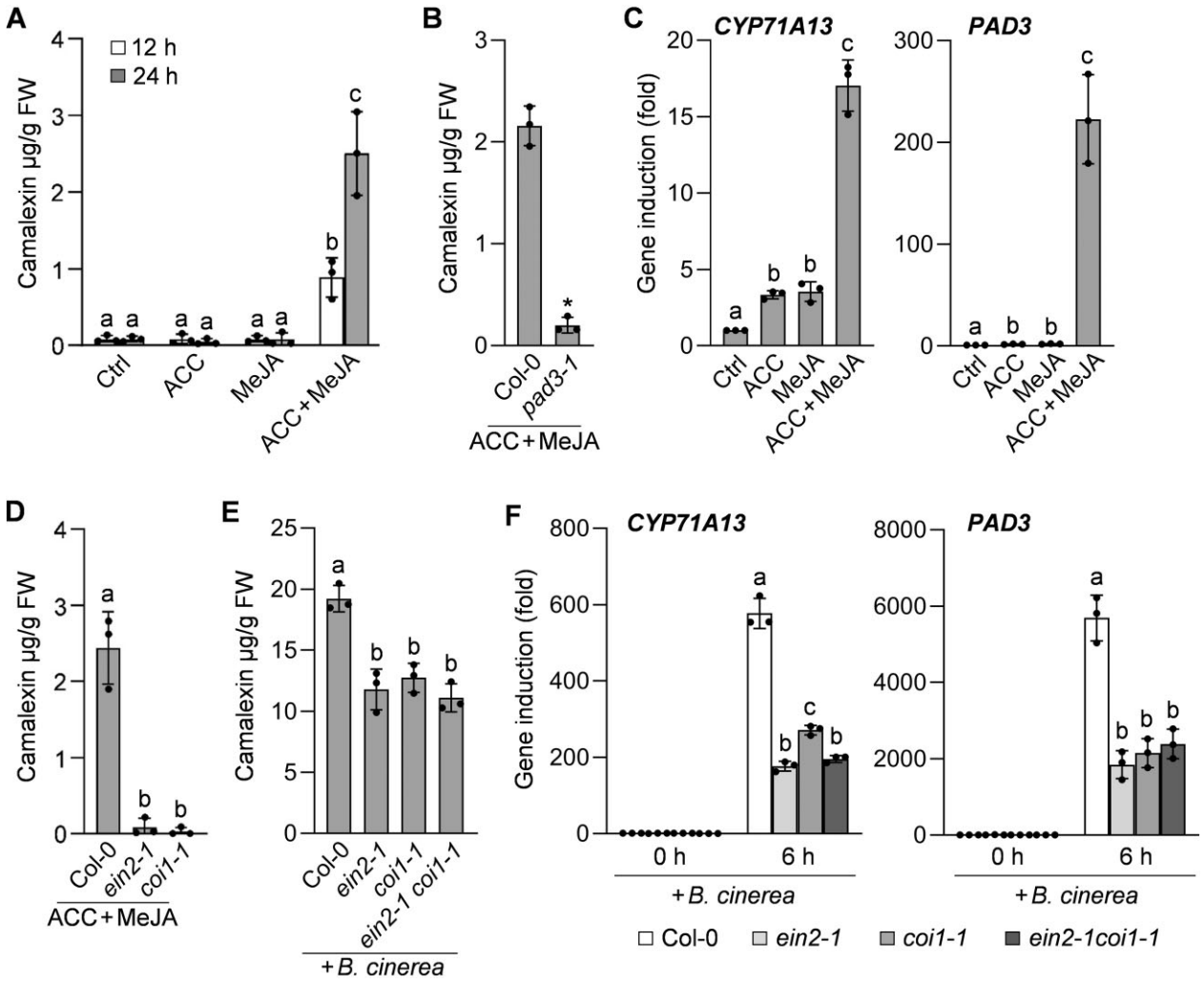

Figure 1 Ethylene and JA pathways synergistically induce camalexin biosynthesis in Arabidopsis. A and B, Cotreatment of Arabidopsis seedlings with ACC and MeJA synergistically induced camalexin biosynthesis. Two-week-old Col-0 (A and B) or *pad3-1* (B) seedlings were treated with 20-µM ACC and/or 50-µM MeJA, or the solvent control (Ctrl) for 24 h in liquid medium, and camalexin production in the medium was quantified. The asterisk above the column indicates significant differences ($P < 0.05$) compared with the Col-0 control (B), as determined by Student's *t* test. C, Cotreatment with ACC and MeJA synergistically activated the expression of camalexin biosynthetic genes. Two-week-old Col-0 seedlings were treated with ACC and/or MeJA as described in (A). The transcript levels of *CYP71A13* and *PAD3* at 24-h posttreatment were analyzed by RT-qPCR. D, Both ethylene and JA signaling pathways are fully required for ACC/MeJA-induced camalexin biosynthesis. Two-week-old Col-0, *ein2-1*, and *coi1-1* seedlings were treated with ACC plus MeJA as described in (A), and camalexin production was quantified. E and F, Both ethylene and JA signaling pathways are involved in the *B. cinerea*-induced camalexin production and camalexin biosynthetic gene activation. Two-week-old Col-0, *ein2-1*, *coi1-1*, and *ein2-1 coi1-1* seedlings were inoculated with *B. cinerea* spores in liquid medium. Camalexin production was measured at 24-h postinoculation (E), and the transcript levels of *CYP71A13* and *PAD3* at the indicated time points were analyzed by RT-qPCR (F). In (A)–(F), error bars indicate standard deviation (SD, $n = 3$ biological repeats), black dots represent individual data points, and different letters above the columns indicate significant differences ($P < 0.05$), as determined by one-way analysis of Variance (ANOVA).

as a crucial positive regulator in *B. cinerea*-induced camalexin biosynthetic gene activation and camalexin production. Additionally, *ERF1* overexpression led to Arabidopsis growth inhibition (Figure 2C), probably due to ERF1-mediated constitutive activation of defense genes such as *PDF1.2* and *PR1* (Supplemental Figure S4). In support of the importance of ERF1-mediated camalexin induction and defense gene activation, the resistance to *B. cinerea* was significantly compromised in *erf1-c1* mutant but was greatly enhanced in *35S:4myc-ERF1* transgenic plants (Supplemental Figures S5 and S6).

Moreover, to test whether chemical induction of *ERF1* expression is sufficient to activate camalexin biosynthesis in the absence of pathogen infection, we generated transgenic Arabidopsis plants (*Est:4myc-ERF1*) expressing 4myc-tagged ERF1 under the control of an estradiol (Est)-inducible promoter. As shown in Figure 2, E and F, Est-induced expression of ERF1 was able to induce camalexin production in *Est:4myc-ERF1* plants without pathogen inoculation. The camalexin induction in *Est:4myc-ERF1* plants after Est treatment was correlated with the activation of camalexin biosynthetic genes *CYP71A13* and *PAD3* (Figure 2G). In

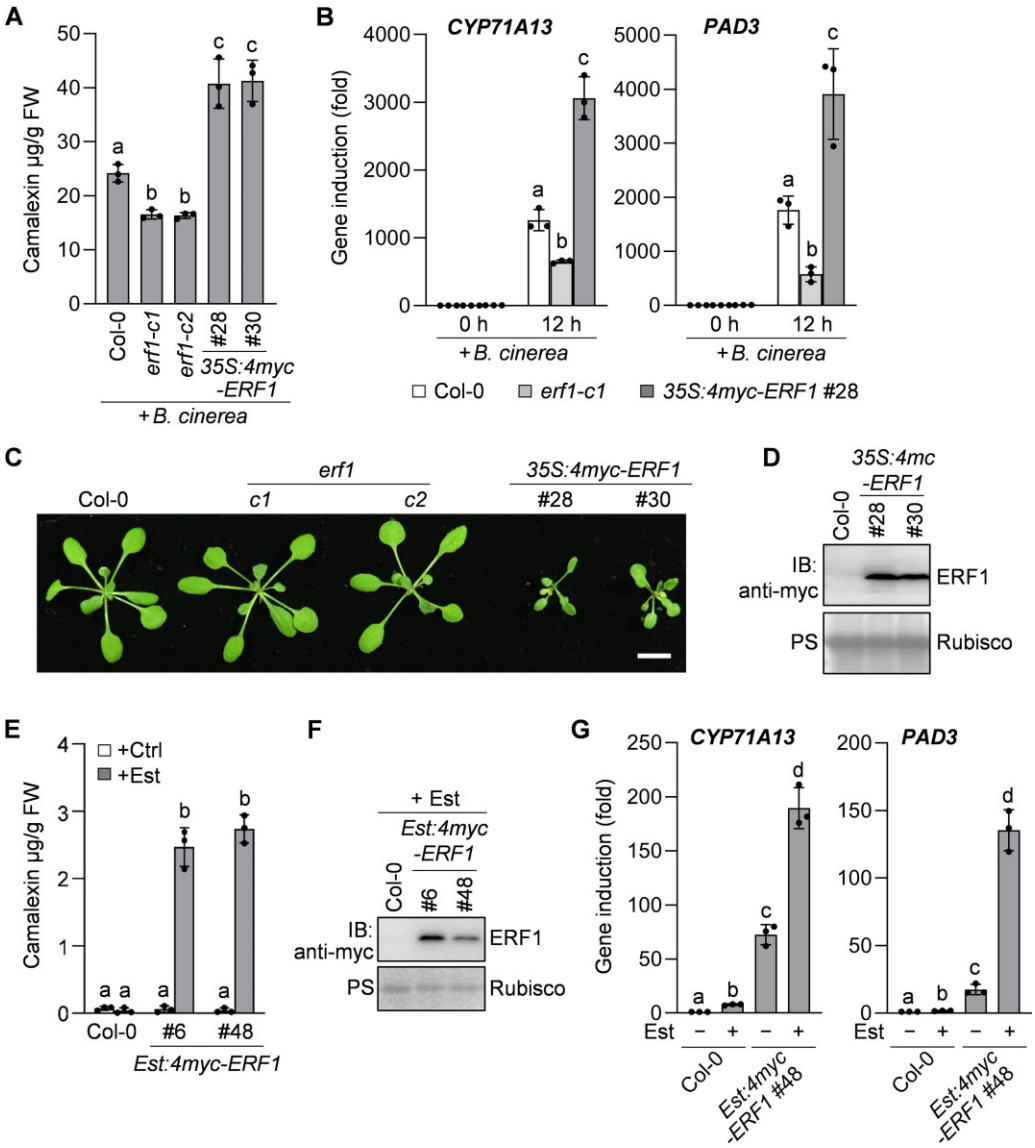

Figure 2 ERF1 is an essential positive regulator of camalexin biosynthesis in Arabidopsis. A and B, ERF1 positively regulates *B. cinerea*-induced camalexin production and camalexin biosynthetic gene expression. Two-week-old seedlings of Col-0, *erf1* mutants and *35S:4myc-ERF1* transgenic lines were inoculated with *B. cinerea* spores. Camalexin production was measured at 24-h postinoculation (A), and the transcript levels of *CYP71A13* and *PAD3* at the indicated time points were analyzed by RT-qPCR (B). C and D, Overexpression of *ERF1* led to growth inhibition of transgenic Arabidopsis plants. Growth phenotypes of 4-week-old Col-0, *erf1* mutants and *35S:4myc-ERF1* transgenic lines grown in soil, scale bar = 1 cm (C). The expression of 4myc-ERF1 was analyzed by IB with anti-myc antibody (D), and total protein loading was assessed by Ponceau S staining (PS). E–G, Est-induced expression of *ERF1* in *Est:4myc-ERF1* transgenic plants induced camalexin production and activated camalexin biosynthetic gene expression. Two-week-old *Est:4myc-ERF1* seedlings were treated with 10 µM Est or the solvent control (Ctrl) for 72 h. Camalexin production was quantified (E). The expression of 4myc-ERF1 was analyzed by IB with anti-myc antibody (F), and the transcript levels of *CYP71A13* and *PAD3* were analyzed by RT-qPCR (G). In (A), (B), (E), and (G), error bars indicate SD ($n = 3$ biological repeats), black dots represent individual data points, and different letters above the columns indicate significant differences ($P < 0.05$), as determined by one-way ANOVA.

contrast, although the WRKY33 transcription factor is also required for pathogen-induced camalexin biosynthetic gene activation and camalexin production (Qiu et al., 2008; Mao et al., 2011), dexamethasone (Dex)-induced expression of WRKY33 was not capable of inducing camalexin biosynthesis in the *Dex:4myc-WRKY33* transgenic plants that express 4myc-tagged WRKY33 under the control of a Dex-inducible promoter (Supplemental Figure S7). Therefore, these data further suggest that ERF1 plays a crucial role in controlling the activation of camalexin biosynthetic genes and the induction of camalexin biosynthesis.

ERF1 integrates the ethylene and JA pathways to directly activate camalexin biosynthetic genes and thereby induce camalexin biosynthesis

We further investigated whether the ethylene and JA pathways synergistically regulate camalexin biosynthesis via ERF1. In line with the function of ERF1 as a downstream

integrator of ethylene and JA signals (Lorenzo et al., 2003), cotreatment of Arabidopsis seedlings with ACC and MeJA synergistically upregulated *ERF1* expression (Figure 3A), while the induction of camalexin biosynthesis by ACC/MeJA cotreatment was largely blocked in the *erf1-c1* mutant (Figure 3B). Consistent with this, the ACC/MeJA-induced activation of camalexin biosynthetic genes *CYP71A13* and *PAD3* were significantly attenuated in *erf1-c1* (Figure 3C), and the ACC/MeJA-induced resistance to *B. cinerea* was largely abolished in *erf1-c1* (Supplemental Figure S5). Therefore, these results indicate that ERF1 is required for the synergistic induction of camalexin biosynthesis and fungal resistance by the ethylene and JA pathways.

Consistent with the important role of ERF1 in *B. cinerea*-induced camalexin biosynthesis (Figure 2A), its expression was highly induced by *B. cinerea* infection (Figure 3D). The *B. cinerea*-induced expression of *ERF1* was largely compromised in both *ein2-1* and *coi1-1* mutants (Figure 3D), indicating the synergistic induction of *ERF1* expression by ethylene and JA in response to *B. cinerea* infection. Notably, overexpression of *ERF1* driven by the *35S* promoter in the *ein2-1 coi1-1* mutant could completely overcome the defect of *ein2-1 coi1-1* in *B. cinerea*-induced camalexin biosynthesis (Figure 3, E and F), indicating that ERF1 acts downstream of ethylene and JA to induce camalexin biosynthesis upon *B. cinerea* infection. Together, the above data demonstrate that ethylene and JA pathways synergistically induce camalexin biosynthesis via ERF1 in response to *B. cinerea* infection.

A luciferase (LUC) reporter-aided analysis of promoter activity in Arabidopsis protoplasts revealed that ERF1 could activate the promoters of camalexin biosynthetic genes *CYP71A13* and *PAD3* (Figure 4, A and B). ERF1 binds the GCC box element (AGCCGCC) to directly regulate defense genes (Solano et al., 1998). A search for GCC boxes in the promoters of *CYP71A13* and *PAD3* found the GCC box-like elements AGCCGAC and AGCCGTC in the promoter regions of *CYP71A13* and *PAD3*, respectively (Figure 4, C and D). Through electrophoresis mobility shift assays (EMSAs), we showed that ERF1 could bind the GCC box-containing regions of both *CYP71A13* and *PAD3* promoters in vitro (Figure 4E). Inclusion of the GCC box-containing but not the GCC box-mutated promoter fragments without biotin labels in the binding reaction of EMSAs effectively competed the binding of ERF1 to the biotin-labeled promoter fragments of *CYP71A13* and *PAD3* (Figure 4E), confirming the specificity of GCC-box binding activities of ERF1 protein. Furthermore, we performed chromatin immunoprecipitation (ChIP)-qPCR analyses using *35S:4myc-ERF1* transgenic plants to test whether ERF1 directly target *CYP71A13* and *PAD3* in vivo. As shown in Figure 4F, compared with the immunoprecipitation using the control IgG antibody, the immunoprecipitation of 4myc-tagged ERF1 protein from *35S:4myc-ERF1* plants using an anti-myc antibody greatly enriched the GCC box-containing regions of both *CYP71A13* and *PAD3* promoters. Therefore, these data indicate that, as a downstream integrator of ethylene and JA pathways, ERF1 directly binds the promoter of camalexin biosynthetic genes *CYP71A13* and *PAD3* to activate their expression, thereby inducing camalexin biosynthesis.

ERF1 and WRKY33 act interdependently and cooperatively to induce camalexin biosynthesis

In addition to ERF1, the transcription factor WRKY33 also directly activates the camalexin biosynthetic genes *CYP71A13* and *PAD3* to induce camalexin biosynthesis in response to *B. cinerea* infection (Qiu et al., 2008; Mao et al., 2011; Birkenbihl et al., 2017). To explore the relationship between ERF1 and WRKY33 in regulating camalexin biosynthesis, we transformed the *35S:4myc-ERF1* construct into the *wrky33-2* mutant background. As shown in Figure 5, B and C, the potentiation of *B. cinerea*-induced camalexin production by *ERF1* overexpression was completely blocked in *35S:4myc-ERF1 wrky33-2* plants compared with that in *35S:4myc-ERF1* plants, although the transgenic ERF1 expression levels were comparable in these different transgenic plants.

The blockage of ERF1-potentiated camalexin biosynthesis in *35S:4myc-ERF1 wrky33-2* plants after *B. cinerea* infection was associated with the dramatically attenuated activation of camalexin biosynthetic genes *CYP71A13* and *PAD3* (Supplemental Figure S8). Consistent with the genetic results, a LUC reporter assay in Arabidopsis protoplasts showed that the activation of *CYP71A13* and *PAD3* promoters by ERF1 was also largely dependent on WRKY33 (Supplemental Figure S9). These results indicate that WRKY33 is required for ERF1-induced camalexin biosynthetic gene activation and camalexin biosynthesis.

Additionally, the inhibition of transgenic plant growth caused by *ERF1* overexpression was also recovered in the *wrky33-2* mutant background (Figure 5, A and B), probably because the ERF1-mediated activation of defense genes such as *PDF1.2* and *PR1* were largely compromised in *35S:4myc-ERF1 wrky33-2* plants (Supplemental Figure S4), indicating that ERF1 also depends on WRKY33 to activate these defense genes. Consistent with the requirement of WRKY33 for ERF1-induced camalexin biosynthesis and defense gene activation, the enhanced resistance to *B. cinerea* observed in *35S:4myc-ERF1* plants was also abolished in *35S:4myc-ERF1 wrky33-2* plants (Supplemental Figure S6).

We further generated the *erf1-c1 wrky33-2* and *erf1-c2 wrky33-2* double mutants to evaluate the relationship between ERF1 and WRKY33 in regulating pathogen-induced camalexin biosynthesis. As shown in Figure 5D and Supplemental Figure S10, the defects of *wrky33-2* in *B. cinerea*-induced camalexin biosynthetic gene activation and camalexin production were more severe than those of *erf1-c1*. However, the camalexin induction levels in *erf1-c1 wrky33-2* and *erf1-c2 wrky33-2* double mutants after *B. cinerea* infection were not further reduced in comparison with that in *wrky33-2* (Figure 5D). Similarly, the *B. cinerea*-induced expression levels of *CYP71A13* and *PAD3* in *erf1-c1 wrky33-2* were comparable with that in *wrky33-2*

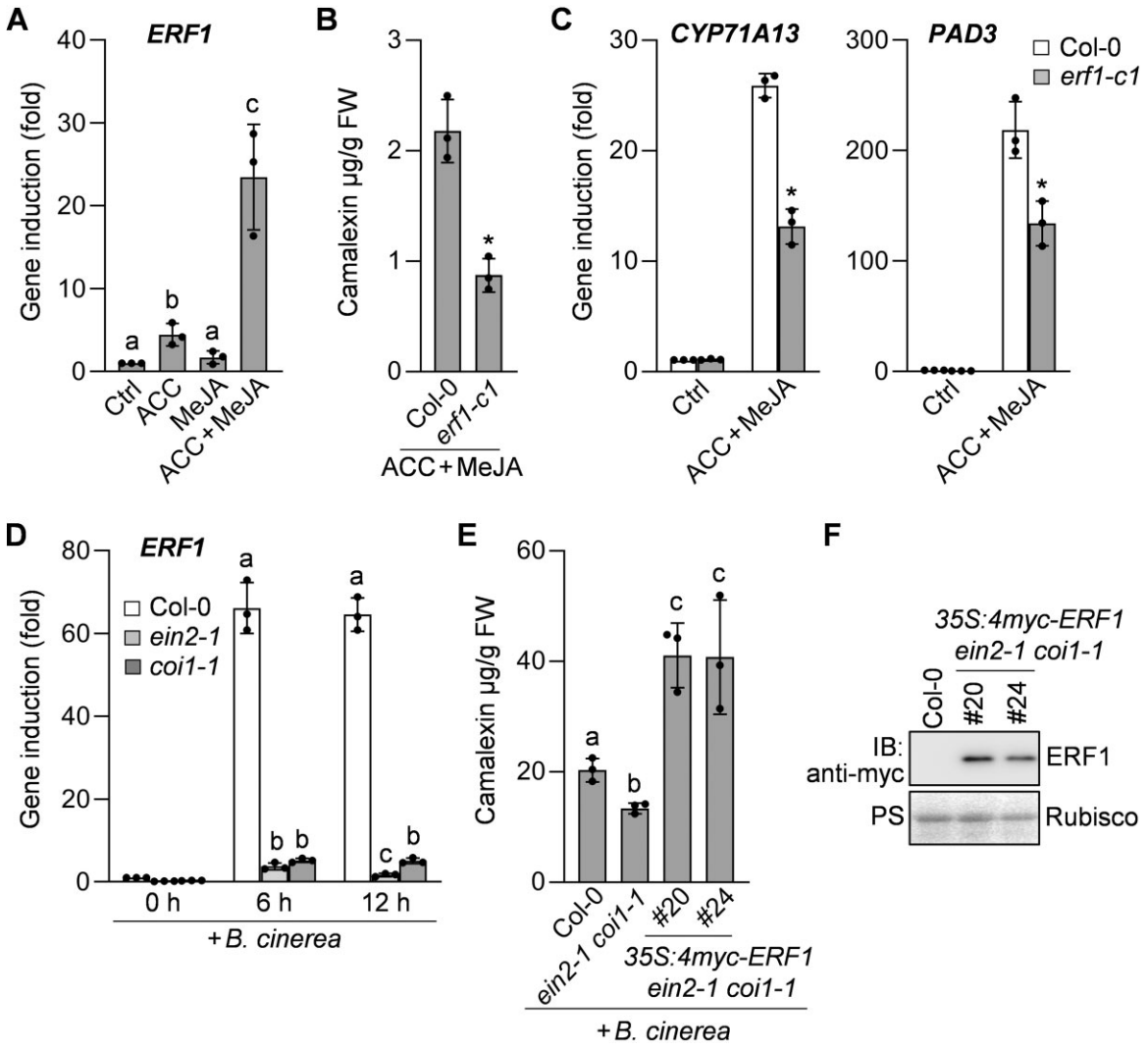

Figure 3 Ethylene and JA pathways act through ERF1 to synergistically induce camalexin biosynthesis. A, Cotreatment of Arabidopsis seedlings with ACC and MeJA synergistically induced *ERF1* expression. Two-week-old Col-0 seedlings were treated with 20-µM ACC and/or 50-µM MeJA, or the solvent control (Ctrl) in liquid medium, and the *ERF1* transcript levels at 24-h posttreatment were analyzed by RT-qPCR. B and C, ERF1 is required for ACC/MeJA-induced camalexin production and camalexin biosynthetic gene activation. Two-week-old Col-0 and *erf1-c1* mutant seedlings were treated with ACC plus MeJA. Camalexin production was measured at 24-h posttreatment (B), and the transcript levels of *CYP71A13* and *PAD3* at 12-h posttreatment were analyzed by RT-qPCR (C). Asterisks above columns indicate significant differences ($P < 0.05$) compared with the Col-0 controls (B, C), as determined by Student's *t* test. D, Both ethylene and JA signaling pathways are required for *B. cinerea*-induced expression of *ERF1*. Two-week-old Col-0, *ein2-1* and *coi1-1* seedlings were inoculated with *B. cinerea* spores. The *ERF1* transcript levels at the indicated time points were analyzed by RT-qPCR. E and F, Overexpression of *ERF1* completely overcame the defect of *ein2-1 coi1-1* in *B. cinerea*-induced camalexin biosynthesis. Two-week-old seedlings of Col-0, *ein2-1 coi1-1* mutant and *35S:4myc-ERF1 ein2-1 coi1-1* transgenic lines were inoculated with *B. cinerea* spores. Camalexin production was measured at 24-h postinoculation (E). The expression of 4myc-ERF1 in *35S:4myc-ERF1 ein2-1 coi1-1* lines was analyzed by IB with anti-myc antibody (F). In (A)–(E), error bars indicate SD ($n = 3$ biological repeats), black dots represent individual data points, and different letters above columns indicate significant differences ($P < 0.05$), as determined by one-way ANOVA.

(Supplemental Figure S10). These results are consistent with the requirement of WRKY33 for ERF1-induced camalexin biosynthetic gene activation and camalexin biosynthesis.

Although the Dex-induced expression of *WRKY33* in *Dex:4myc-WRKY33* plants was unable to induce camalexin biosynthesis in the absence of pathogen infection (Supplemental Figure S7), overexpression of *WRKY33* in *35S:4myc-WRKY33* plants substantially enhanced *B. cinerea*-responsive camalexin induction (Figure 5E). To investigate whether ERF1 is required for the WRKY33-induced camalexin production in response to *B. cinerea* infection, we transformed the *35S:4myc-WRKY33* construct into the *erf1-c1* mutant. As shown in Figure 5, E and F, the enhancement of *B. cinerea*-responsive camalexin induction by *WRKY33* overexpression was largely abolished in *35S:4myc-WRKY33 erf1-c1* plants compared with that in *35S:4myc-WRKY33* plants, although the transgenic WRKY33 expression levels were comparable in these different transgenic plants, indicating that ERF1 is also required for WRKY33-induced camalexin biosynthesis in response to *B. cinerea* infection.

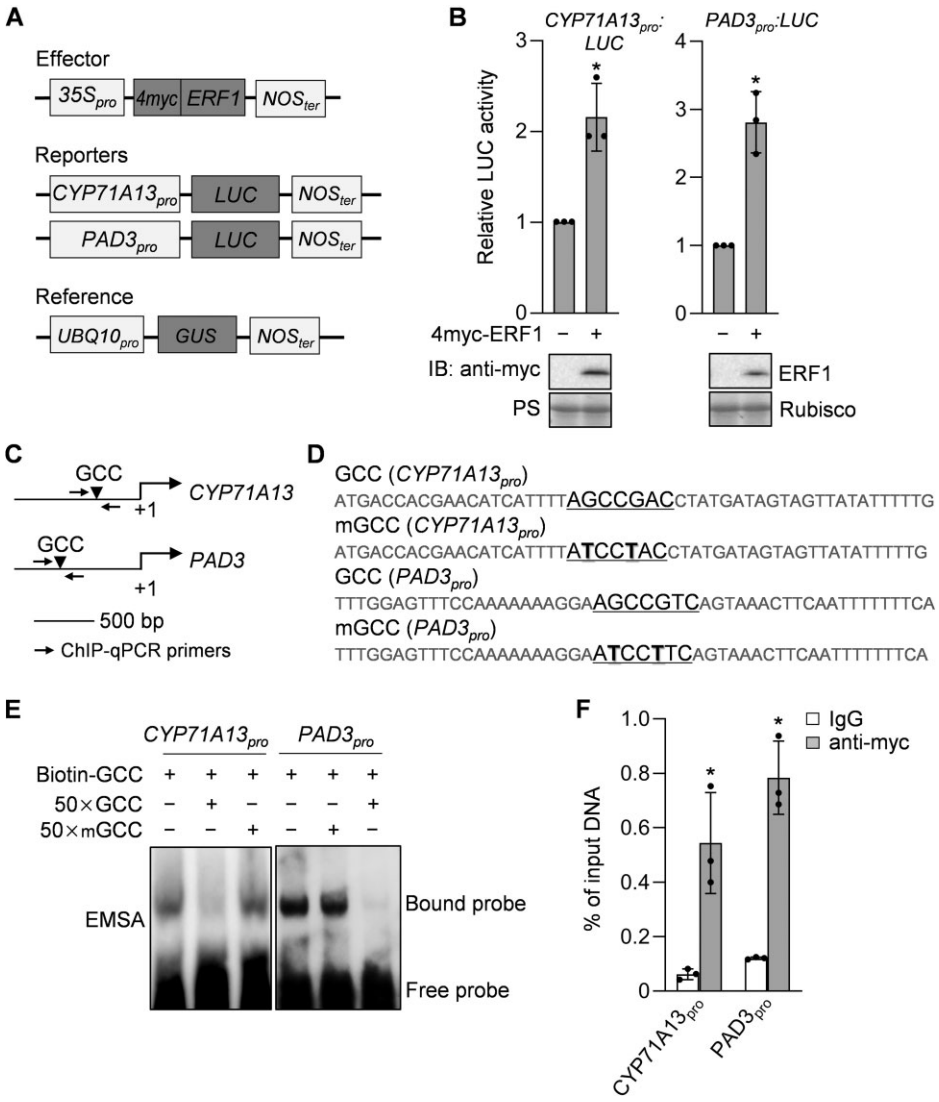

Figure 4 ERF1 directly activates camalexin biosynthetic genes. A, Schematic diagrams of the effector, reporter, and reference constructs used in the *LUC* reporter-aided analysis of *CYP71A13* and *PAD3* promoter activities in Arabidopsis protoplasts. B, Expression of ERF1 induced the activation of camalexin biosynthetic gene promoters in Arabidopsis protoplasts. The reporter construct *CYP71A13pro:LUC* or *PAD3pro:LUC* was cotransfected with the effector construct *35S:4myc-ERF1* or the vector control (Ctrl) into protoplasts. The reference construct *UBQ10pro:GUS* was included in all transfections and served as an internal transfection control. The LUC activities were normalized to GUS activities, and the data are shown as relative fold increases over the controls. Protein levels of 4myc-ERF1 in transfected protoplasts were analyzed by IB with anti-myc antibody. C, Schematic diagrams showing the GCC box-like elements in the promoters of *CYP71A13* and *PAD3*. Small arrows indicate the primers used for ChIP-qPCR analysis in (F). D, The wild-type and mutated oligonucleotide sequences of the GCC box-containing probes (abbreviated as GCC and mGCC) derived from *CYP71A13* and *PAD3* promoters. The underlined sequences indicate the GCC box elements. The mutated nucleotides in the probes are highlighted in boldface. E, ERF1 binds the GCC box-containing probes derived from *CYP71A13* and *PAD3* promoters in vitro. EMSA was performed using the recombinant MBP-ERF1-HA protein and the biotin-labeled probes as shown in (D). The specificity of probe binding activities was demonstrated by the competition assays using 50-fold excess of the unlabeled wild-type or mutated probes. F, ERF1 binds to the GCC-box-containing regions of *CYP71A13* and *PAD3* promoters in vivo. ChIP-qPCR was performed using *35S:4myc-ERF1* transgenic seedlings. The ERF1–chromatin complex was immunoprecipitated using anti-myc antibody and protein G-agarose. A control reaction was performed using mouse IgG. ChIP- and input-DNA samples were quantified by qPCR using primers as shown in (C). The ChIP results are presented as percentage of input DNA. In (B) and (F), error bars indicate SD ($n = 3$ biological repeats), black dots represent individual data points, and asterisks above columns indicate significant differences ($P < 0.05$) compared with the respective controls, as determined by Student's *t* test.

Furthermore, we transformed the *Est:4myc-ERF1* construct into the *35S:4myc-WRKY33* transgenic background to assess the relationship between ERF1 and WRKY33 in regulating camalexin biosynthesis. As shown in Figure 5, G and H, in the absence of pathogen infection, the ERF1-induced camalexin biosynthesis in *Est:4myc-ERF1 35S:4myc-WRKY33* plants was substantially enhanced by overexpression of *WRKY33*, compared with that in *Est:4myc-ERF1* plants, although the Est-induced ERF1 expression levels were comparable in these different transgenic plants, suggesting the cooperation of

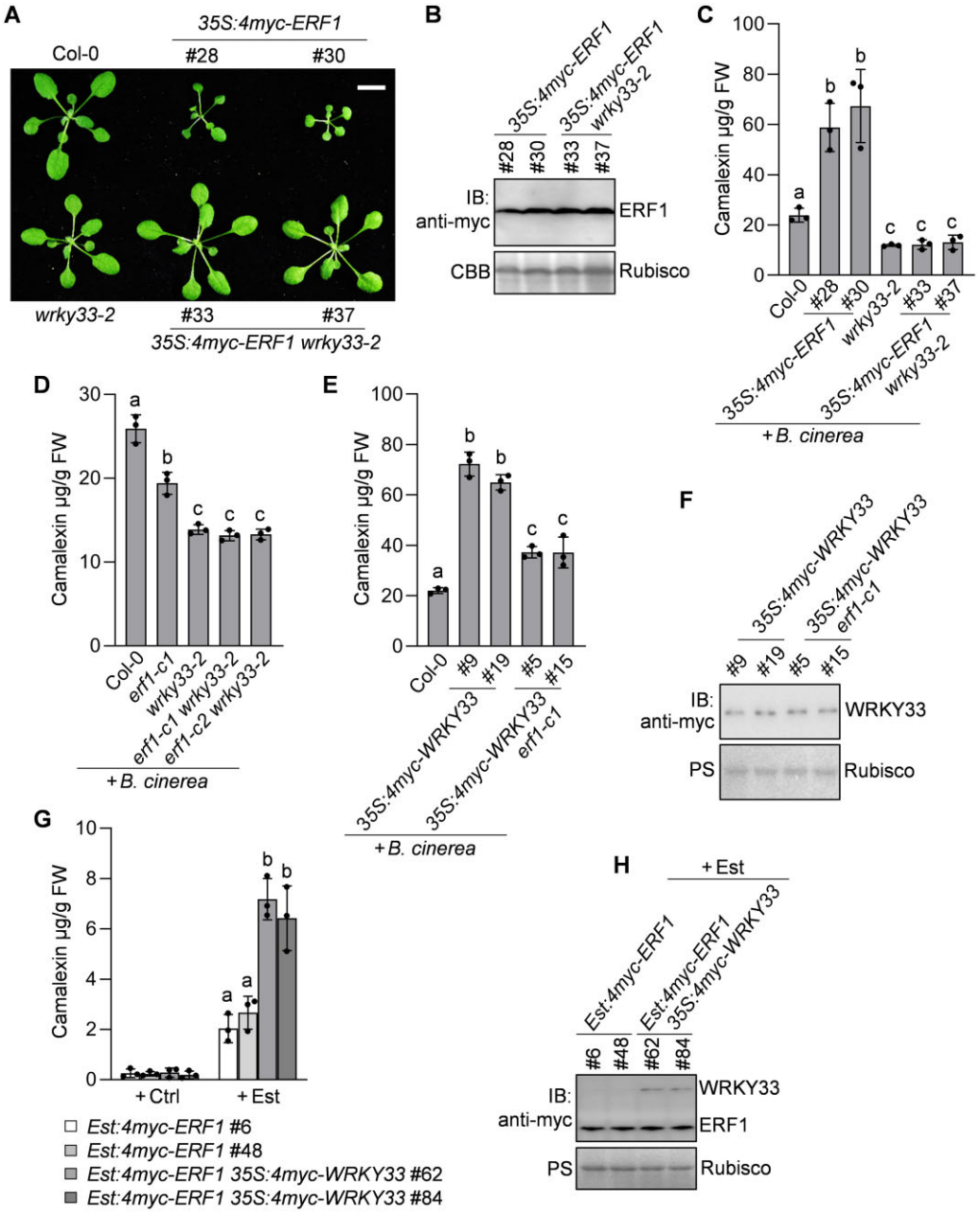

Figure 5 ERF1 and WRKY33 function interdependently and cooperatively to induce camalexin biosynthesis. A and B, The transgenic plant growth inhibition caused by *ERF1* overexpression was recovered in the *wrky33-2* background. Growth phenotypes of 4-week-old Col-0, *wrky33-2*, *35S:4myc-ERF1*, and *35S:4myc-ERF1 wrky33-2* plants grown in soil, scale bar = 1 cm (A). The expression of 4myc-ERF1 in *35S:4myc-ERF1* and *35S:4myc-ERF1 wrky33-2* plants was analyzed by IB with anti-myc antibody (B). C, WRKY33 is required for ERF1-mediated potentiation of camalexin biosynthesis in response to *B. cinerea* infection. Two-week-old Col-0, *wrky33-2*, *35S:4myc-ERF1*, and *35S:4myc-ERF1 wrky33-2* seedlings were inoculated with *B. cinerea* spores. Camalexin production was measured at 24-h postinoculation. D, The *erf1-c1 wrky33-2* and *wrky33-2* mutants exhibited similar levels of defects in *B. cinerea*-induced camalexin biosynthesis. The analyses of *B. cinerea*-induced camalexin production in the indicated genotypes were performed as described in (C). E and F, Overexpression of *WRKY33* led to the ERF1-dependent potentiation of camalexin biosynthesis in response to *B. cinerea* infection. The *B. cinerea*-induced camalexin production (E) and the expression of 4myc-WRKY33 in the indicated genotypes were analyzed as described in (C) and (B), respectively. G and H, Overexpression of *WRKY33* enhanced the ERF1-induced camalexin biosynthesis in the absence of pathogen infection. Two-week-old *Est:4myc-ERF1* and *Est:4myc-ERF1 35S:4myc-WRKY33* transgenic seedlings were treated with 10 µM Est or the solvent control (Ctrl) for 72 h. Camalexin production was quantified (G), and the expression of 4myc-ERF1 and 4myc-WRKY33 was analyzed by IB (H). In (C), (D), (E), and (G), error bars indicate SD (n = 3 biological repeats), black dots represent individual data points, and different letters above the columns indicate significant differences ($P < 0.05$), as determined by one-way ANOVA.

ERF1 and WRKY33 in activating camalexin biosynthesis. Consistent with this, a LUC reporter assay showed that coexpression of ERF1 and WRKY33 could additively activate *CYP71A13* and *PAD3* promoters in Arabidopsis protoplasts (Supplemental Figure S11). Taken together, the above data indicate that ERF1 and WRKY33 act in an interdependent and cooperative manner to activate camalexin biosynthetic genes and induce camalexin biosynthesis.

ERF1 interacts with WRKY33 in the nucleus

To reveal the mechanism underlying the interdependence of ERF1 and WRKY33 in inducing camalexin biosynthesis, we tested whether ERF1 and WRKY33 regulate each other's expression. As shown in Supplemental Figure S12, the *B. cinerea*-induced expression of *ERF1* or *WRKY33* were not affected in *wrky33-2* or *erf1-c1* mutant, respectively, indicating that these two transcription factors do not regulate each other's expression in response to *B. cinerea* infection.

We further investigated whether ERF1 and WRKY33 function together through direct interaction. As shown in an in vitro pull-down assay, the hexa-histidine ($6\times$His)-tagged WRKY33 was pulled down by GST-tagged ERF1 but not by GST itself (Figure 6A). Consistent with this, in a coimmunoprecipitation (Co-IP) assay using Arabidopsis protoplasts, HA-tagged WRKY33 (WRKY33-HA) was coimmunoprecipitated with 4Myc-tagged ERF1 by anti-myc agarose from transfected protoplasts (Figure 6B). In addition, when WRKY33-HA was transiently coexpressed with GFP-tagged ERF1 (ERF1-GFP) in *Nicotiana benthamiana*, it could also be coimmunoprecipitated with ERF1-GFP by anti-GFP agarose in Co-IP analyses (Figure 6C). Therefore, the pull-down and Co-IP analyses indicate that ERF1 interacts with WRKY33 in vitro and in vivo.

Furthermore, we also performed a split yellow fluorescence protein (YFP)-based bimolecular fluorescence complementation (BiFC) assay in Arabidopsis protoplasts to confirm and visualize the ERF1–WRKY33 interaction. As shown in the BiFC analyses (Figure 6D), a clear YFP signal was observed in the nucleus when ERF1 and WRKY33 fused with the N- and C-terminal half of YFP, respectively, were coexpressed in protoplasts, indicating that the interaction of ERF1 and WRKY33 occurs in the nucleus.

Given the requirement of WRKY33 for ERF1-mediated activation of *CYP71A13* and *PAD3* (Supplemental Figures S8 and S9), these protein–protein interaction analyses suggest that ERF1 forms transcriptional complexes with WRKY33 in the nucleus to cooperatively activate camalexin biosynthetic genes and induce camalexin biosynthesis. Notably, a recently study also reported the identification of hypoxia-responsive ERF–WRKY transcriptional complexes, including the ERF1–WRKY53 complex in Arabidopsis and the DkERF24–DkWRKY1 complex in persimmon (*Diospyros kaki*; Zhu et al., 2019), suggesting that the formation of ERF-WRKY complexes may represent a general mechanism for ERF- and WRKY-mediated activation of stress-responsive genes.

ERF1 is phosphorylated by MPK3/MPK6 in vitro and in vivo

During the characterization of ERF1 function, we detected two bands of the ERF1-GFP fusion protein when it was expressed in Arabidopsis protoplasts (Figure 7A). Upon treatment with the λ protein phosphatase (λPPase), the upper band disappeared (Figure 7A), indicating that it represents the phosphorylated form of ERF1-GFP protein. A further examination of ERF1 protein sequence revealed a cluster of three potential MAPK phosphorylation sites (Ser-8, 14, 22, three serines followed by prolines) in the N-terminus (Figure 7B). Similarly, WRKY33 contains clustered proline-directed serines (SP cluster) in its N-terminal domain (Figure 7B), which were demonstrated to be the phosphorylation sites of MPK3 and MPK6 (Mao et al., 2011). Therefore, we tested whether MPK3 and MPK6 phosphorylate ERF1 on its N-terminal SP cluster. As shown in Figure 7, C and D, in vitro phosphorylation analyses using the phosphate-affinity probe Phostag-Biotin showed that the active MPK3/MPK6 indeed could phosphorylate the ERF1 N-terminal region ($ERF1_N$) containing the SP cluster but not the rest of the protein ($ERF1_{DB+C}$) containing the AP2/ERF DNA-binding domain and the C-terminus of ERF1. Another phosphorylation assay using γ-^{32}P-labeled ATP confirmed the in vitro phosphorylation of $ERF1_N$ but not $ERF1_{DB+C}$ by MPK3/MPK6 (Figure 7E). Mutating Ser-8 to Ala (S8A) but not Ser-14 or Ser-22 to Ala (S14A or S22A) in $ERF1_N$ largely blocked its phosphorylation by MPK3/MPK6, while the $ERF1_N$ mutant with all these three Ser mutated to Ala (3SA) completely lost its phosphorylation by MPK3/MPK6 (Figure 7F). Therefore, these in vitro phosphorylation analyses indicate that MPK3/MPK6 phosphorylate ERF1 on its N-terminal SP cluster, in which Ser-8 is likely the major site phosphorylated by MPK3/MPK6.

To further demonstrate the phosphorylation of ERF1 by MPK3/MPK6 in vivo, the GFP-tagged wild-type ERF1 and its loss-of-phosphorylation mutant ($ERF1^{3SA}$-GFP) and phospho-mimic mutant ($ERF1^{3SD}$-GFP, with Ser-8/14/22 all mutated to Asp) were expressed in Arabidopsis protoplasts; meanwhile, a constitutively active version of MKK5 ($MKK5^{T215D/S221D}$, abbreviated as $MKK5^{DD}$) was coexpressed to activate its downstream MPK3 and MPK6. As shown in Figure 7G, without $MKK5^{DD}$-activated MPK3/MPK6, a portion of ERF1-GFP protein was already phosphorylated, probably by the basally activated MPK3/MPK6 during protoplast preparation. Upon activation of MPK3/MPK6 by the coexpressed $MKK5^{DD}$, the phosphorylated portion of ERF1-GFP protein was significantly increased, indicating that the activated MPK3/MPK6 phosphorylated ERF1 in protoplasts. Notably, the $ERF1^{3SA}$-GFP mutant protein completely lost both the basal and the $MKK5^{DD}$-induced phosphorylation band, whereas the phospho-mimic $ERF1^{3SD}$-GFP protein exhibited constitutively up-shifted band corresponding to the phosphorylated ERF1-GFP band, indicating that the Ser-8/14/22 residues of ERF1 also serve as the MPK3/MPK6 phosphorylation sites in protoplasts. Together, these data

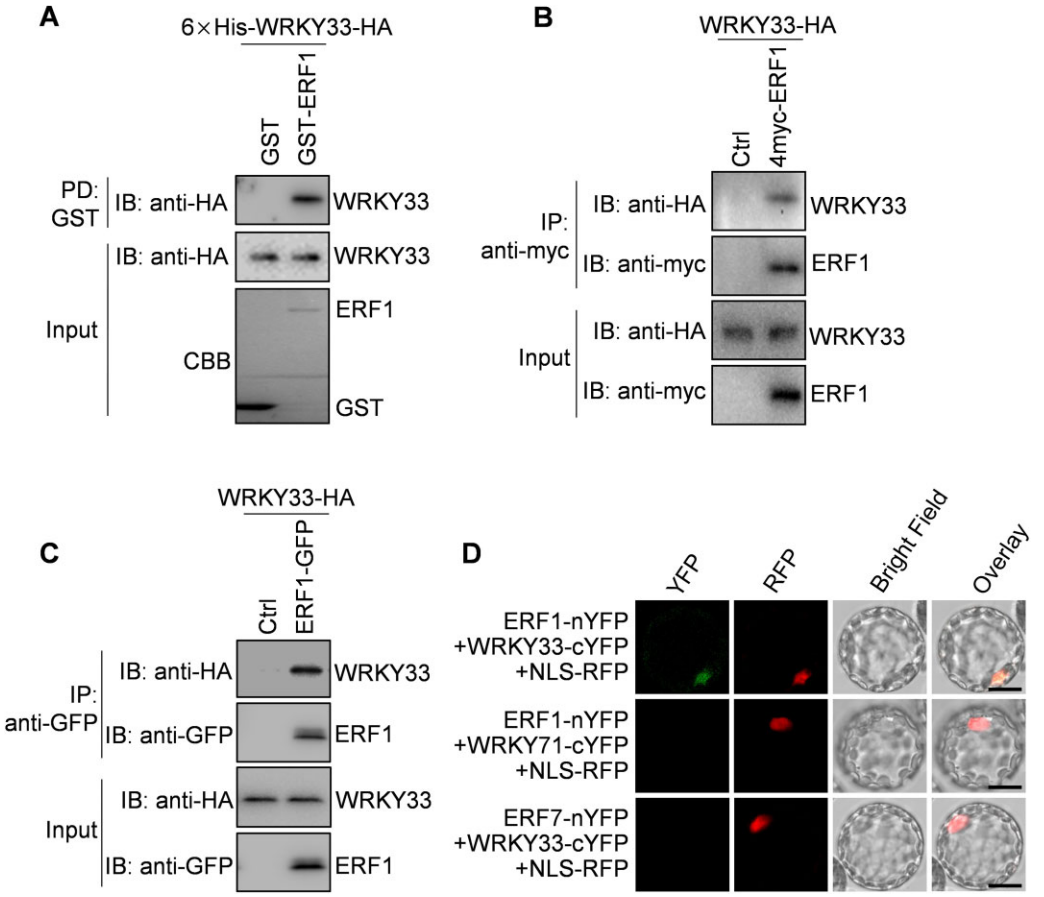

Figure 6 ERF1 interacts with WRKY33 in vitro and in vivo. A, ERF1 interacts with WRKY33 in an in vitro pull-down assay. GST- or GST-ERF1-bound glutathione beads were incubated with 6 × His-WRKY33-HA proteins, and the pulled-down (PD) proteins were analyzed by IB with anti-HA antibody (IB: anti-HA; top). The protein inputs were assessed by IB (middle) and Coomassie Brilliant Blue staining (bottom). B, ERF1 associates with WRKY33 in Arabidopsis protoplasts. 4myc-ERF1 and WRKY33-HA proteins were coexpressed in protoplasts. The proteins immunoprecipitated from protoplast extracts using anti-myc agarose beads (IP: anti-myc) were analyzed by IB with anti-HA (IB: anti-HA) or anti-myc antibody (IB: anti-myc; top two panels). The protein inputs were assessed by IB (bottom two parts). Ctrl, vector control. C, ERF1 associates with WRKY33 in *N. benthamiana*. ERF1-GFP and WRKY33-HA proteins were transiently coexpressed in *N. benthamiana* leaves. Co-IP analyses were performed using anti-GFP agarose beads, similarly as described in (B). D, ERF1 interacts with WRKY33 in the nucleus. BiFC assays were performed by expressing the indicated combinations of proteins in Arabidopsis protoplasts, with WRKY71-cYFP and ERF7-nYFP proteins coexpressed as negative controls. The fluorescence was observed under a confocal microscope. The NLS-RFP protein was coexpressed to visualize the protoplast nuclei. Scale bars = 25 μm.

indicate that MPK3/MPK6 also phosphorylate ERF1 on its N-terminal SP cluster in vivo.

MPK3 and MPK6 play redundant roles in regulating Arabidopsis immunity (Meng and Zhang, 2013) and the *mpk3 mpk6* double mutant is embryo lethal. To further provide direct evidence supporting the MPK3/MPK6-mediated phosphorylation of ERF1 during plant–pathogen interaction, we used a conditional *mpk3 mpk6* double mutant, *mpk3 mpk6 pMPK6:MPK6*^{Y144G}, whose embryonic lethality was rescued by a transgene of the chemical 4-amino-1-tert-butyl-3-(1′-naphthyl)pyrazolo[3,4-*d*]pyrimidine (NA-PP1)-sensitized version of MPK6 (MPK6^{Y144G}; Xu et al., 2014). The kinase activity of MPK6^{Y144G} in *mpk3 mpk6 pMPK6:MPK6*^{Y144G} plants can be specifically inhibited by NA-PP1, a derivative of the PP1 (4-amino-1-tert-butyl-3-(4-methylphenyl)pyrazolo[3,4-*d*]pyrimidine) kinase inhibitor with a bulky side chain, which, therefore, cannot enter the ATP binding pocket of a normal kinase (Bishop et al., 2000; Xu et al., 2014). To compare the phosphorylation of ERF1 in *mpk3 mpk6 pMPK6:MPK6*^{Y144G} and Col-0 backgrounds, the ERF1-GFP fusion protein was expressed in the protoplasts of these two plants. The transfected protoplasts were pretreated with NA-PP1 and then treated with the chitin oligomer chitooctaose, a representative fungal PAMP. As shown in Figure 7H, the chitin-induced phosphorylation of ERF1-GFP was blocked in the protoplasts of *mpk3 mpk6 pMPK6:MPK6*^{Y144G} but not Col-0 upon pretreatment with NA-PP1 that specifically inhibits the activity of MPK6^{Y144G}, indicating that MPK3/MPK6 mediate the phosphorylation of ERF1 in Arabidopsis upon perception of PAMPs/pathogens.

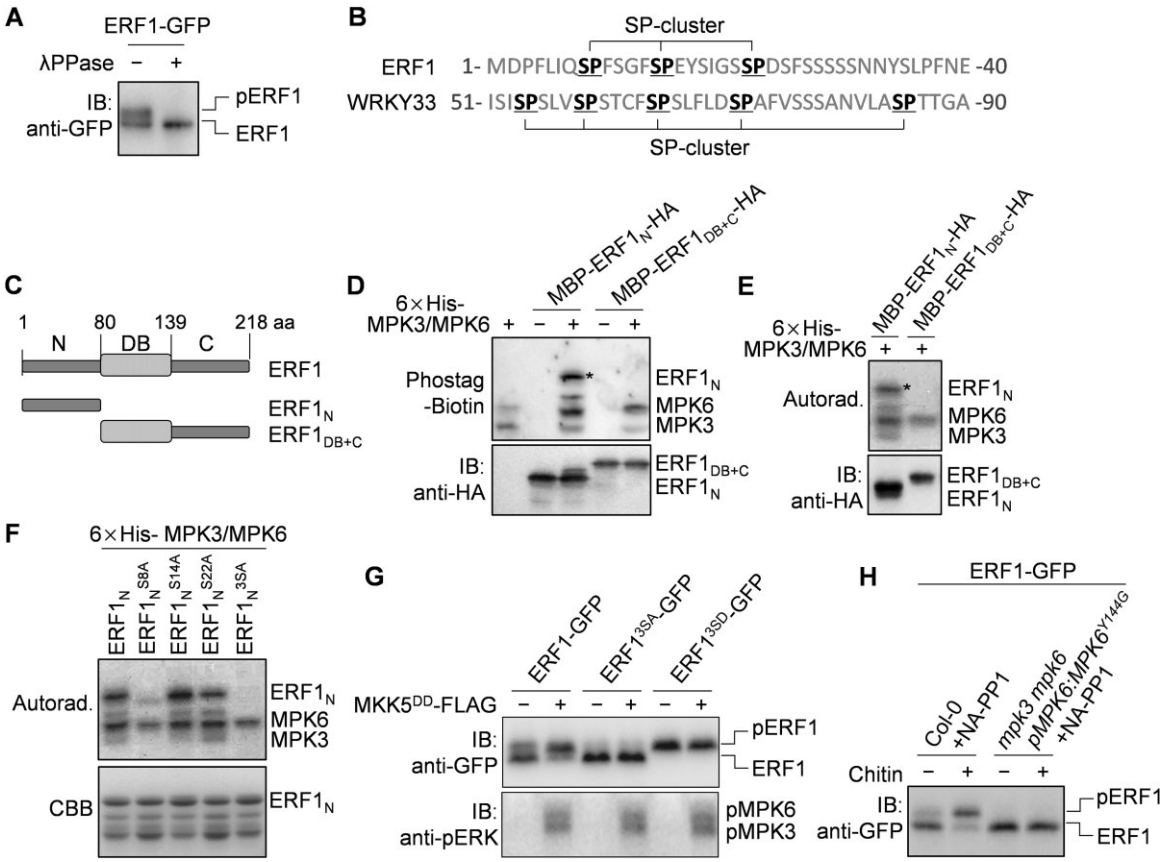

Figure 7 In vitro and in vivo phosphorylation of ERF1 by MPK3/MPK6. A, ERF1 was phosphorylated in Arabidopsis protoplasts. ERF1-GFP protein was expressed in Arabidopsis protoplasts and immunoprecipitated from protoplast extracts using anti-GFP agarose beads. The immunoprecipitated ERF1-GFP was treated with or without λ protein phosphatase (λPPase) and then analyzed by IB. B, Putative MAPK phosphorylation sites in the N-terminus of ERF1 and the identified MPK3/MPK6 phosphorylation sites in the N terminus of WRKY33. C, Schematic diagrams showing the domain architectures of wild-type and truncated ERF1 proteins. The AP2/ERF DNA-binding domain of ERF1 ($ERF1_{DB}$) is located in its central region. The amino acid positions are labeled on the top. The truncated fragments of ERF1 used for phosphorylation analyses are shown at the bottom. D and E, The N-terminal domain of ERF1 ($ERF1_N$) was phosphorylated by MPK3/MPK6. The phosphorylation reactions without (D) or with (E) the addition of [γ-^{32}P]ATP were performed using the MBP/HA-tagged ERF1 fragments as substrates and the 6 × His-MPK3/MPK6 activated by 6 × His-$MKK5^{DD}$ as the kinase. After separation by SDS–PAGE, the phosphorylated proteins were detected using the Phostag-Biotin probe (D) or by autoradiography (Autorad. [E]; top). The protein inputs were assessed by IB (bottom). Asterisks indicate the phosphorylated MBP-$ERF1_N$-HA protein. F, MPK3/MPK6 phosphorylate the N-terminal serine residues of ERF1. The single and triple Ser-to-Ala mutants of MBP-$ERF1_N$-HA protein were purified and their ability to be phosphorylated by MPK3/MPK6 was analyzed by in vitro phosphorylation assays as described in (E). G, Mutation of the N-terminal serine residues in ERF1 blocked its phosphorylation by MPK3/MPK6 in Arabidopsis protoplasts. The wild-type ERF1-GFP protein or its mutant with the three N-terminal Ser mutated to Ala (3SA) or Asp (3SD) were coexpressed with $MKK5^{DD}$-Flag in protoplasts. The phosphorylation of ERF1-GFP proteins and the activation of MPK3/MPK6 by $MKK5^{DD}$ were analyzed by IB using anti-GFP and anti-phospho-ERK1/2 (anti-pERK) antibodies, respectively. H, MPK3/MPK6 mediated the chitin-induced phosphorylation of ERF1 in Arabidopsis protoplasts. The ERF1-GFP protein was expressed in the protoplasts of Col-0 and *mpk3 mpk6 pMPK6:MPK6*^{Y144G} plants. The transfected protoplasts were pretreated with NA-PP1 to block the activation of $MPK6^{Y144G}$ and then treated with the chitin oligomer chitooctaose to induce the phosphorylation of ERF1-GFP, which was further analyzed by IB. Ctrl, solvent control.

MPK3/MPK6-mediated phosphorylation of ERF1 enhances its transactivation activity

We next investigated the effect of MPK3/MPK6-mediated phosphorylation on ERF1 activity. The MPK3/MPK6-phosphorylated SP cluster is located in ERF1 N-terminus and is far away from its DNA-binding domain (Figure 7, B and C), suggesting that MPK3/MPK6-mediated phosphorylation is unlikely to regulate the DNA-binding activity of ERF1. To evaluate whether phosphorylation of the ERF1 N-terminal SP cluster by MPK3/MPK6 regulates ERF1 transactivation activity in Arabidopsis protoplasts, we generated three *35S* promoter-driven effector constructs expressing wild-type ERF1, the loss-of-phosphorylation $ERF1^{3SA}$ or the phosphomimic $ERF1^{3SD}$ protein fused with the DNA binding domain of the yeast transcription factor GAL4 (GAL4DB-ERF1-HA, GAL4DB-$ERF1^{3SA}$-HA, and GAL4DB-$ERF1^{3SD}$-HA) (Figure 8A). To perform transactivation assays, Arabidopsis protoplasts were cotransfected with one of the effector constructs and a reporter construct harboring the *LUC* reporter gene under the control of a synthetic promoter consisting of the

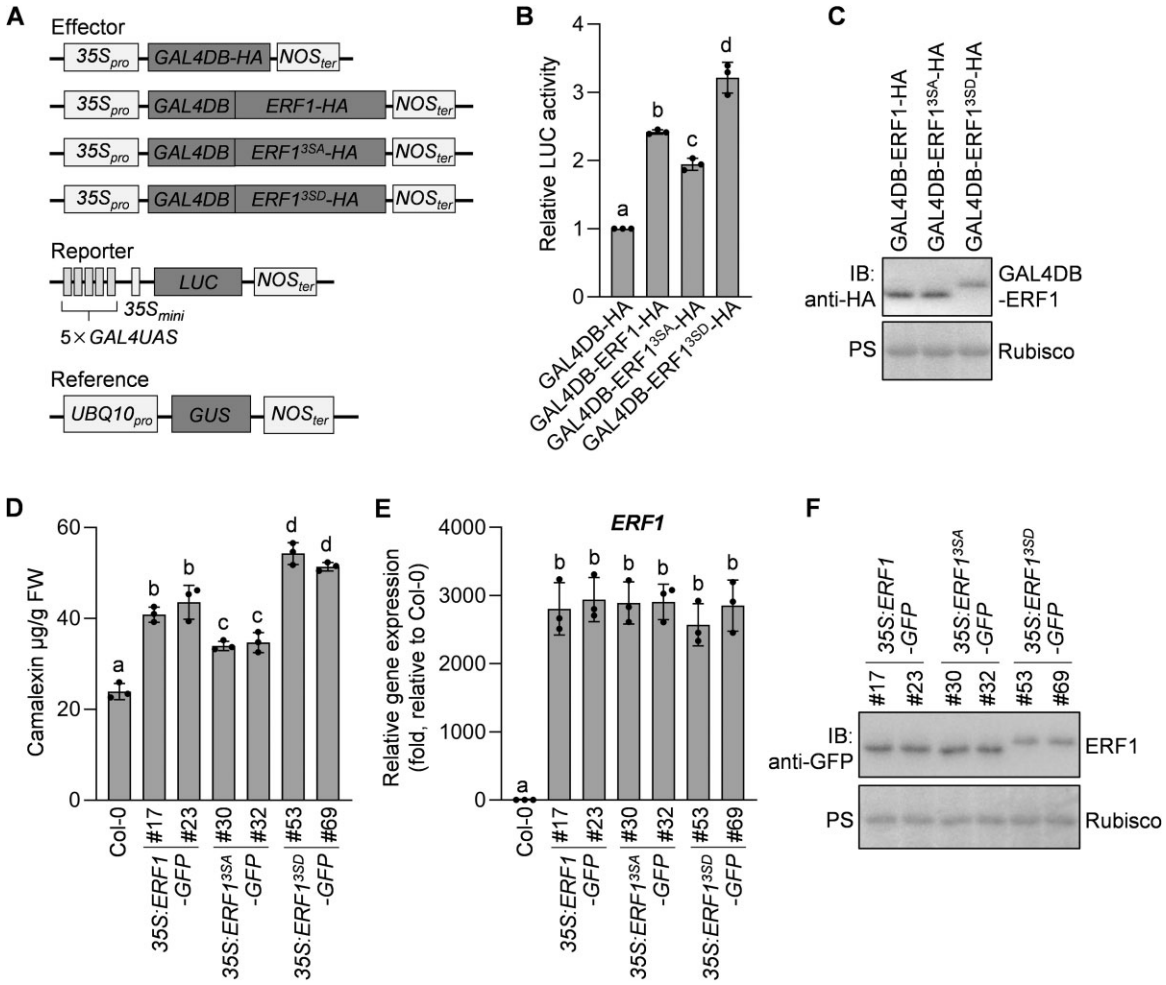

Figure 8 Phosphorylation of ERF1 by MPK3/MPK6 enhances ERF1 transactivation activity. A, Schematic diagrams of the effector, reporter, and reference constructs used in the transactivation assays. The reporter construct contains the *LUC* reporter gene driven by a synthetic promoter consisting of five repeats of *GAL4UAS* and the *35S* minimal promoter ($35S_{mini}$). In the effector constructs, GAL4DB-HA alone or fused with ERF1^{3SA} or ERF1^{3SD} was expressed under the control of the *35S* promoter. B and C, Phosphorylation of ERF1 increased its transactivation activity in Arabidopsis protoplasts. The reporter construct and one of the effector constructs were cotransfected into protoplasts. The reference construct $UBQ10_{pro}$:*GUS* was included in all transfections and served as an internal transfection control. The LUC activities were normalized to the GUS activities, and the data are shown as relative fold increases over the background from the transfection with the *35S:GAL4DB-HA* construct (B). The expression of GAL4DB-ERF1-HA, GAL4DB-ERF1^{3SA}-HA, and GAL4DB-ERF1^{3SD}-HA proteins was analyzed by IB using anti-HA antibody (C). D–F, Phosphorylation of ERF1 enhanced its activity in potentiating *B. cinerea*-induced camalexin biosynthesis in Arabidopsis transgenic plants. Two-week-old seedlings of Col-0 and the indicated transgenic lines were inoculated with *B. cinerea* spores. Camalexin production was measured at 24-h postinoculation (D). The *ERF1* transcript levels in transgenic lines were analyzed by RT-qPCR (E), and the levels of ERF1-GFP, ERF1^{3SA}-GFP and ERF1^{3SD}-GFP proteins in transgenic lines were analyzed by IB (F). In (B), (D), and (E), error bars indicate SD (n = 3 biological repeats), black dots represent individual data points, and different letters above the columns indicate significant differences ($P < 0.05$), as determined by one-way ANOVA.

GAL4-specific upstream activation sequence (*GAL4UAS*) and the 35S minimal promoter (Figure 8A). As shown in Figure 8, B and C, when expressed at comparable levels in Arabidopsis protoplasts, GAL4DB-ERF1^{3SD}-HA exhibited significantly higher transactivation activity than GAL4DB-ERF1-HA, whereas GAL4DB-ERF1^{3SA}-HA showed significantly lower transactivation activity than GAL4DB-ERF1-HA, as indicated by the LUC activities induced by these ERF1 fusion proteins, suggesting that phosphorylation of the ERF1 N-terminal SP cluster increased the transactivation activity of ERF1.

We also generated the transgenic plants overexpressing ERF1-GFP, ERF1^{3SA}-GFP or ERF1^{3SD}-GFP protein (*35S:ERF1-GFP*, *35S:ERF1^{3SA}-GFP*, and *35S:ERF1^{3SD}-GFP*) to assess the effect of ERF1 phosphorylation on its activity in potentiating *B. cinerea*-induced camalexin biosynthesis. As shown in Figure 8, D–F, in transgenic lines with comparable levels of transgene expression, *35S:ERF1^{3SD}-GFP* lines produced significantly increased levels of camalexin than *35S:ERF1-GFP* lines, whereas *35S:ERF1^{3SA}-GFP* lines produced significantly reduced levels of camalexin than *35S:ERF1-GFP* lines, when these transgenic lines were infected by *B. cinerea*, indicating

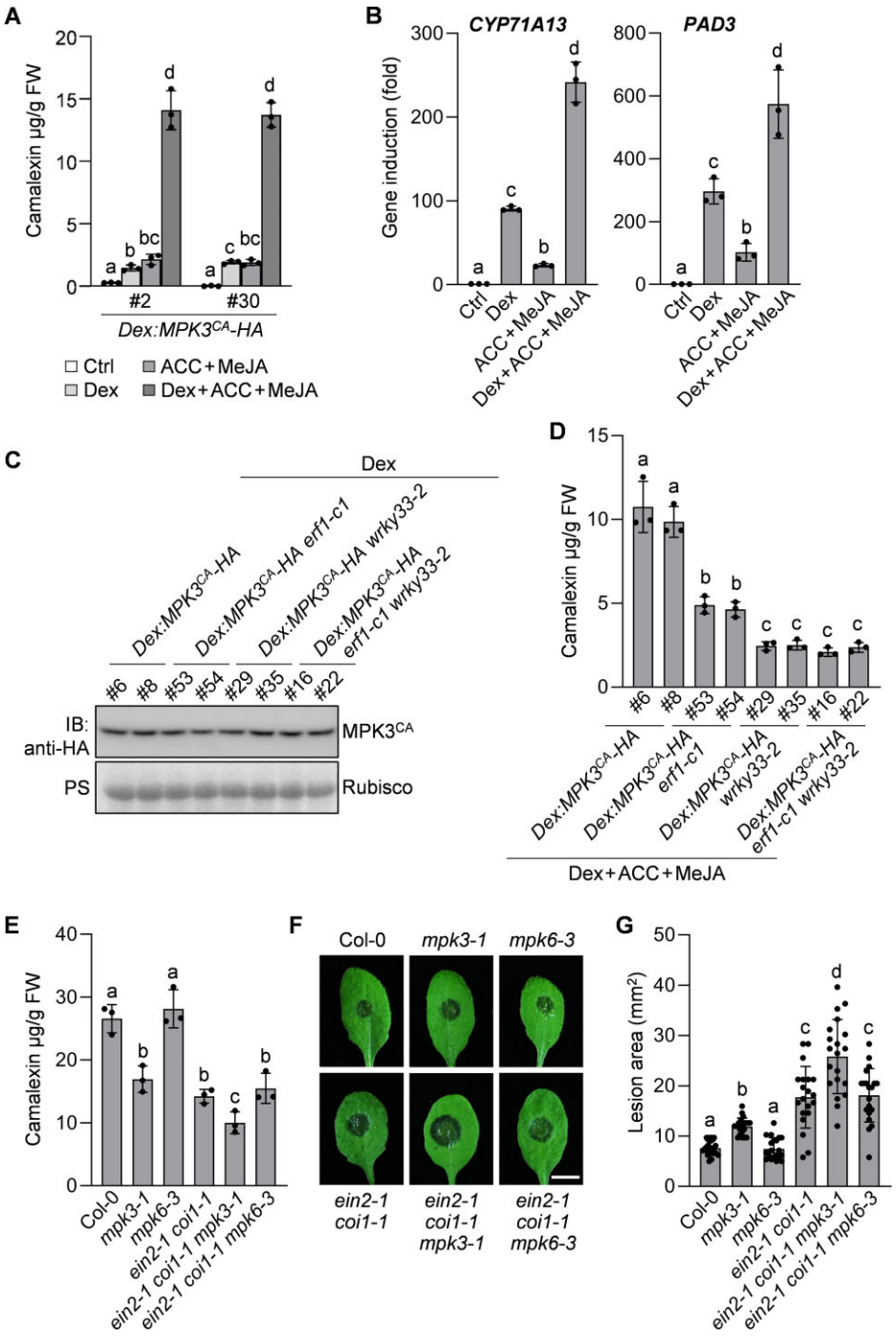

Figure 9 Synergistic regulation of camalexin biosynthesis and *B. cinerea* resistance by MPK3 and ethylene/JA signaling pathways. A and B, MPK3 and ethylene/JA pathways synergistically induce camalexin production and camalexin biosynthetic gene activation. Two-week old *Dex:MPK3*^{CA}*-HA* transgenic seedlings were treated with 5-µM Dex for 12-h and/or 20-µM ACC plus 50-µM MeJA for 24 h. Camalexin production was measured (A), and the transcript levels of *CYP71A13* and *PAD3* were analyzed by RT-qPCR (B). C and D, ERF1 and WRKY33 mediate the synergistic induction of camalexin biosynthesis by MPK3 and ethylene/JA pathways. Two-week-old seedlings of the indicated transgenic lines were treated with 5 µM Dex for 12 h and 20-µM ACC plus 50-µM MeJA for 24 h. Camalexin production was measured (D), and the expression of MPK3^{CA}-HA protein was analyzed by IB (C). E, MPK3 and ethylene/JA pathways contribute additively to *B. cinerea*-induced camalexin production. Camalexin produced from 2-week-old Col-0 and mutant seedlings indicated was measured at 24 h postinoculation with *B. cinerea* spores. F and G, Additive contribution of MPK3 and ethylene/JA pathways to *B. cinerea* resistance. Fully developed leaves of 4-week-old Col-0 and mutant plants indicated were inoculated with droplets of *B. cinerea* spore suspension. Leaf images were taken at 48-h postinoculation, scale bar = 5 mm (F). Meanwhile, lesion size was quantified (G). In (A), (B), (D), (E), and (G), error bars indicate SD ([A], [B], [D], and [E]: $n = 3$ biological repeats; [G]: $n = 20$ leaves from different plants of each genotype), black dots represent individual data points, and different letters above the columns indicate significant differences ($P < 0.05$), as determined by one-way ANOVA.

that phosphorylation of ERF1 enhanced its activity in inducing camalexin biosynthesis. Of note, the relatively weak abilities of GAL4DB-ERF1^{3SA}-HA protein to activate *LUC* reporter gene in protoplasts (Figure 8, A–C) and ERF1^{3SA}-GFP protein to enhance *B. cinerea*-induced camalexin biosynthesis in transgenic plants (Figures 8, D–F) indicate that ERF1^{3SA} still has a relatively weak transcriptional activity. Therefore, the above results collectively suggest that the activity of ERF1 does not totally depend on its phosphorylation by MPK3/MPK6 but can be significantly enhanced by MPK3/MPK6-mediated phosphorylation. Additionally, in independent transgenic lines with comparable levels of *ERF1-GFP*, *ERF1^{3SA}-GFP*, or *ERF1^{3SD}-GFP* transcripts (Figure 8E), the accumulation levels of ERF1^{3SA}-GFP and ERF1^{3SD}-GFP proteins were also comparable with those of ERF1-GFP protein (Figure 8F), suggesting that phosphorylation of ERF1 by MPK3/MPK6 does not regulate the stability of ERF1 protein.

Ethylene, JA, and MPK3 signaling pathways synergistically regulate camalexin biosynthesis and *B. cinerea* resistance

The finding that MPK3/MPK6 phosphoactivate ERF1 promoted us to investigate whether MPK3/MPK6 and ethylene/JA signaling pathways act through ERF1 to synergistically regulate camalexin biosynthesis and disease resistance.

To this end, based on a previous report about constitutively active MAPK versions (Berriri et al., 2012), we generated *Dex:MPK3^{CA}-HA* transgenic Arabidopsis plants expressing a HA-tagged constitutively active version of MPK3 (MPK3$^{D193G/E197A}$, named MPK3^{CA}) under the control of a Dex-inducible promoter. Following treatment with Dex and/or ACC/MeJA, we compared the levels of camalexin production in *Dex:MPK3^{CA}-HA* plants. As shown in Figure 9A, upon treatment with Dex, the level of camalexin induction by Dex-induced MPK3^{CA} was comparable to that induced by treatment with ACC/MeJA. Notably, cotreatment of *Dex:MPK3^{CA}-HA* plants with Dex and ACC/MeJA showed a synergistic effect on inducing camalexin production, resulting in a camalexin induction level much higher than that induced by either Dex or ACC/MeJA treatment. The synergistic induction of camalexin biosynthesis upon Dex and ACC/MeJA cotreatment was associated with higher levels of *CYP71A13* and *PAD3* induction by the cotreatment (Figure 9B). These results indicate that MPK3 and ethylene/JA signaling pathways synergistically induce camalexin biosynthetic gene activation and camalexin biosynthesis.

To further determine whether the synergistic induction of camalexin biosynthesis by MPK3 and ethylene/JA pathways is mediated by ERF1 and WRKY33, we transformed the *Dex:MPK3^{CA}-HA* construct into the *erf1-c1*, *wrky33-2*, and *erf1-c1 wrky33-2* mutant backgrounds (Figure 9C). As shown in Figure 9, C and D, upon cotreatment with Dex and ACC/MeJA, the levels of camalexin production synergistically induced by MPK3^{CA} and ACC/MeJA in *Dex:MPK3^{CA}-HA erf1-c1*, *Dex:MPK3^{CA}-HA wrky33-2* and *Dex:MPK3^{CA}-HA erf1-c1 wrky33-2* transgenic lines were all largely reduced in comparison with that in *Dex:MPK3^{CA}-HA* lines, although the Dex-induced MPK3^{CA} expression levels were comparable in these different transgenic lines, indicating that both ERF1 and WRKY33 are required for the synergistic induction of camalexin biosynthesis by MPK3 and ethylene/JA pathways. Notably, the MPK3^{CA}/ACC/MeJA-induced camalexin production in *Dex:MPK3^{CA}-HA erf1-c1 wrky33-2* lines was not further reduced in comparison with those in *Dex:MPK3^{CA}-HA wrky33-2* lines (Figure 9D), which is consistent with the coaction of ERF1 and WRKY33 in a transcriptional complex (Figure 6). Therefore, these data indicate that ERF1 and WRKY function together to mediate the synergistic induction of camalexin biosynthesis by MPK3 and ethylene/JA pathways.

Furthermore, to provide loss-of-function evidence supporting the MPK3/MPK6- and ethylene/JA-mediated synergistic regulation of pathogen-induced camalexin biosynthesis, we generated the *ein2-1 coi1-1 mpk3-1* and *ein2-1 coi1-1 mpk6-3* triple mutants and compared the camalexin induction levels in these triple mutants with those in the parental single and double mutants after *B. cinerea* infection. Again, compromised camalexin production was observed in *ein2-1 coi1-1* (Figure 9E). The *B. cinerea*-induced camalexin production was also compromised in *mpk3-1*, but not in *mpk6-3*, and was further reduced in *ein2-1 coi1-1 mpk3-1*, but not in *ein2-1 coi1-1 mpk6-3*, compared with that in *ein2-1 coi1-1* (Figure 9E). These results indicate that ethylene/JA and MPK3 signaling pathways also act synergistically to positively regulate *B. cinerea*-induced camalexin biosynthesis. Based on a previous report (Ren et al., 2008), the absence of camalexin induction defects caused by *MPK6* mutation in different backgrounds is likely due to the redundancy of *MPK3/MPK6* and the relatively minor contribution of *MPK6* in regulating camalexin biosynthesis.

Consistent with the finding of ethylene/JA- and MPK3-mediated synergistic regulation of camalexin biosynthesis, we also observed an additive contribution of the ethylene/JA and MPK3 pathways to Arabidopsis resistance against *B. cinerea* infection. As shown in Figure 9, F and G, compared with Col-0 plants, the *ein2-1 coi1-1* and *mpk3-1* mutants displayed increased susceptibility to *B. cinerea*, while the *ein2-1 coi1-1 mpk3-1* triple mutant showed even stronger susceptibility. The increased *B. cinerea* susceptibility in these mutants was closely correlated with their reduced camalexin production (Figure 9, E–G), highlighting the importance of camalexin production for Arabidopsis resistance to *B. cinerea*. Therefore, both gain- and loss function evidence indicates that ethylene/JA pathways function synergistically with MPK3 to positively regulate camalexin biosynthesis and *B. cinerea* resistance, which is consistent with the cooperative regulation of ERF1 by ethylene/JA and MPK3 at transcriptional and posttranscriptional levels.

Discussion

Pathogen-induced phytoalexin production is an integral part of plant immunity and plays a critical role in plant disease

resistance (Piasecka et al., 2015). The biosynthetic pathways of several phytoalexins have been elucidated (Sonderby et al., 2010; Geu-Flores et al., 2011; Piasecka et al., 2015), but the signaling pathways regulating their biosynthesis remain largely elusive. As the most prominent phytoalexin in Arabidopsis, camalexin is essential for Arabidopsis resistance to a number of fungal and oomycetic pathogens (Glazebrook and Ausubel, 1994; Thomma et al., 1999; Bednarek et al., 2009; Schlaeppi et al., 2010; Stotz et al., 2011; Hiruma et al., 2013). Previously, we characterized the regulation of pathogen-induced camalexin biosynthesis by MPK3/MPK6 and their downstream transcription factor WRKY33 (Mao et al., 2011; Zhou et al., 2020). In this study, we revealed that ethylene and JA signaling pathways act synergistically with the MPK3/MPK6–WRKY33 signaling module at multiple levels to induce camalexin biosynthesis in response to *B. cinerea* infection (Figures 1, 9, and 10). We found that the ERF1 transcription factor integrates ethylene and JA pathways to directly activate camalexin biosynthetic genes, thereby inducing camalexin biosynthesis (Figures 2, 3, and 4). ERF1 was further found to interact with WRKY33, meanwhile these two transcription factors were shown to act interdependently in the induction of camalexin biosynthesis (Figures 5 and 6; Supplemental Figures S8–S11), suggesting that ERF1 forms transcriptional complexes with WRKY33 to cooperatively induce camalexin biosynthesis. Interestingly, as an integrator of ethylene and JA pathways, ERF1 was also identified as a substrate of MPK3/MPK6 (Figure 7), which phosphorylate ERF1 to enhance its transactivation activity (Figure 8), suggesting that ERF1 mediates the synergy of ethylene/JA and MPK3/MPK6 signaling pathways to activate camalexin biosynthesis. Indeed, both gain- and loss-of-function analyses demonstrated the synergistic induction of camalexin biosynthesis by ethylene/JA and MPK3 signaling pathways (Figure 9).

Taken together, based on these results, we propose a model in which ethylene, JA, and MPK3/MPK6 signaling pathways act synergistically to induce camalexin biosynthesis via multilayered regulatory mechanisms (Figure 10). In this model, ethylene and JA pathways synergistically induce camalexin biosynthesis via transcriptional activation of *ERF1* gene, while MPK3/MPK6 act synergistically with ethylene/JA pathways via phosphoactivating ERF1 activity. At the promoters of camalexin biosynthetic genes, ERF1 and WRKY33 are proposed to form transcriptional complexes to cooperatively activate camalexin biosynthetic genes. The ERF1–WRKY33 transcriptional complexes may act through facilitating the recruitment of RNA polymerase and/or its

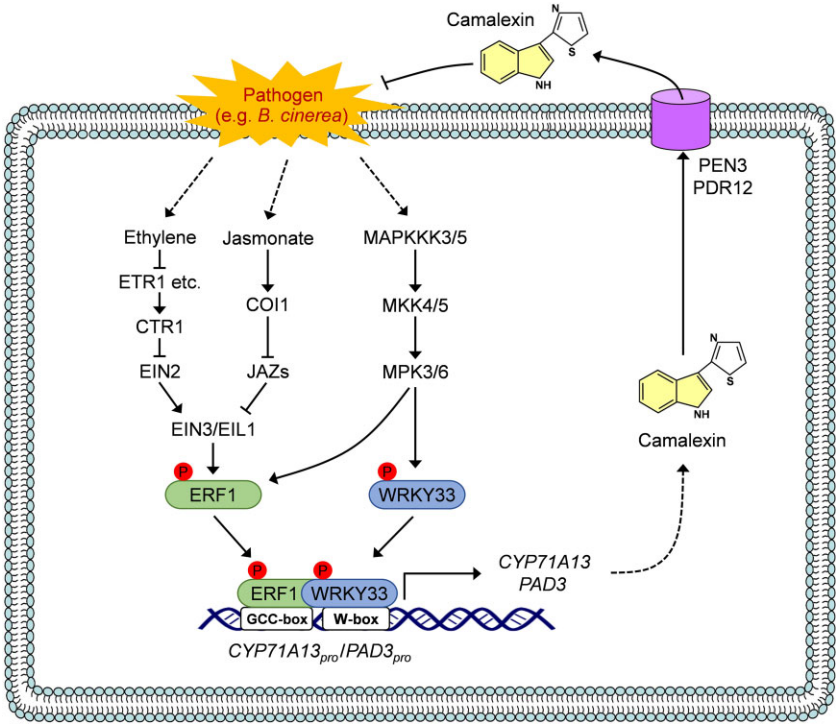

Figure 10 A model depicting the multilayered synergistic regulation of pathogen-induced camalexin biosynthesis by ethylene, JA and MPK3/MPK6 signaling pathways in Arabidopsis. In response to pathogen (e.g. *B. cinerea*) infection, ethylene and JA signaling pathways act synergistically to induce camalexin biosynthesis via transcriptional activation of *ERF1* gene. ERF1 directly binds to the promoters of camalexin biosynthetic genes and forms transcriptional complexes with WRKY33, thereby cooperating with WRKY33 to activate camalexin biosynthetic genes and induce camalexin biosynthesis. MPK3/MPK6 phosphorylate ERF1 to enhance its transactivation activity and therefore act synergistically with ethylene/JA pathways via ERF1 to induce camalexin biosynthesis. Since MPK3/MPK6 also phosphoactivate WRKY33 to induce camalexin biosynthesis, the interaction and cooperation of ERF1 and WRKY33 could also mediate the synergy of ethylene/JA and MPK3/MPK6 signaling pathways to induce camalexin biosynthesis. The induced camalexin is finally exported to the extracellular space by the transporters PEN3 and PDR12 to defend against pathogens.

associated factors to activate the transcription of camalexin biosynthetic genes. Given that MPK3/MPK6 also phosphoactivate WRKY33 to induce camalexin biosynthesis (Mao et al., 2011; Zhou et al., 2020), the formation of the ERF1–WRKY33 transcriptional complex would also mediate the synergy of ethylene/JA and MPK3/MPK6 signaling pathways in activating camalexin biosynthesis. Since both ERF1 and WRKY33 are also required for the bacterium *P. syringae* pv. *tomato* DC3000 (*Pst* DC3000)-induced camalexin production in Arabidopsis (Supplemental Figure S13), the ERF1–WRKY33 complex is likely involved in activating camalexin biosynthesis in response to both fungal and bacterial pathogens. Notably, a recent study also reported the identification of ERF–WRKY transcriptional complexes, including the Arabidopsis ERF1–WRKY53 complex and the persimmon DkERF24–DkWRKY1 complex, both of which are involved in regulating hypoxia-responsive genes (Zhu et al., 2019). Therefore, this study together with the previous report suggests that the formation of ERF–WRKY complexes may represent a general mechanism for ERF- and WRKY-mediated activation of stress-responsive genes.

Interestingly, although ERF1 and WRKY33 act interdependently and cooperatively to induce camalexin biosynthesis, chemically induced expression of *ERF1* but not *WRKY33* induced camalexin production in transgenic Arabidopsis plants without pathogen infection (Supplemental Figure S7). We propose that this unexpected result could be due to a dramatic difference in the basal expression levels of *ERF1* and *WRKY33*. As shown in Supplemental Figure S14, in the absence of pathogen infection, the basal transcript level of *WRKY33* is ~10-fold higher than that of *ERF1*, which probably would result in a much higher basal protein level of WRKY33 than ERF1 in Arabidopsis plants. Under this circumstance, the transgenically overexpressed ERF1 can form ERF1–WRKY33 transcriptional complexes with a relatively high basal level of WRKY33 protein to induce camalexin biosynthesis in the absence of pathogen attack (Supplemental Figure S7). Conversely, a low basal level of ERF1 protein may be inadequate to form a threshold level of ERF1–WRKY33 transcriptional complexes with the transgenically overexpressed WRKY33 for inducing camalexin biosynthesis in the absence of pathogen infection (Supplemental Figure S7). This hypothesis is also consistent with the observation that overexpression of *ERF1* and *WRKY33* together showed an additive effect on the induction of camalexin biosynthesis in transgenic Arabidopsis plants without pathogen infection (Figure 5, G and H). However, in contrast to the inability of *WRKY33* overexpression to induced camalexin biosynthesis in the absence of pathogen attack (Supplemental Figure S7), overexpression of *WRKY33* could substantially enhance the *B. cinerea*-induced camalexin biosynthesis (Figure 5E), probably because the expression of endogenous *ERF1* is induced to a high level upon *B. cinerea* infection (Figure 3D).

In addition to ethylene/JA pathways, we recently showed that the CDPKs CPK5 and CPK6 function cooperatively with MPK3/MPK6 to positively regulate camalexin biosynthesis via differential phosphorylation of WRKY33 (Zhou et al., 2020). Of note, different from MPK3/MPK6, CPK5 cannot phosphorylate ERF1 (Supplemental Figure S15), suggesting that CPK5/CPK6 do not act through ERF1 to interact with ethylene/JA pathways in upregulating camalexin biosynthesis. However, the phosphoactivation of WRKY33 by CPK5/CPK6 can potentially mediate the synergy of CPK5/CPK6 and ethylene/JA pathways via the WRKY33–ERF1 transcriptional complex to activate camalexin biosynthesis. In this way, ethylene, JA, MPK3/MPK6, and CPK5/CPK6 signaling pathways will constitute a regulatory network via ERF1 and WRKY33 to induce camalexin biosynthesis synergistically.

Besides ERF1 and WRKY33, several other transcription factors including MYB51, MYB122, ERF72, and NAC042 are also involved in the induction of camalexin biosynthesis in response to pathogen attack (Saga et al., 2012; Frerigmann et al., 2015; Yang et al., 2020; Li et al., 2022). Additionally, a recent study reports that the histone modification-mediated epigenetic activation of camalexin biosynthetic genes is implicated in the induction of pathogen-responsive camalexin biosynthesis (Zhao et al., 2021). Therefore, in addition to ethylene/JA and MPK3/MPK6 signaling pathways and their downstream ERF1 and WRKY33 transcription factors reported here, the pathogen-induced camalexin biosynthesis is also regulated by multiple other pathways and transcription factors, which probably contribute to the residual camalexin induction in *ein2-1 coi1-1 mpk3-1* and *erf1-c wrky33-2* mutants upon *B. cinerea* infection (Figures 5D and 9E).

In this study, MPK3/MPK6 was shown to positively regulate ethylene signaling via phosphoactivation of ERF1, a key transcription factor in ethylene signaling pathways. Previously, biochemical and genetic analyses in Arabidopsis demonstrated that MPK3/MPK6 also positively regulate the pathogen-responsive ethylene biosynthesis through phosphorylation and stabilization of the ACC synthase (ACS) isoforms, ACS2 and ACS6, two rate-limiting enzymes for pathogen-induced ethylene biosynthesis (Liu and Zhang, 2004; Han et al., 2010; Li et al., 2012). Interestingly, MPK3/MPK6 was also shown to positively regulate the expression of *ACS2* and *ACS6* genes via phosphoactivating WRKY33, which directly activates *ACS2*/*ACS6* expression to induce ethylene biosynthesis (Li et al., 2012). Therefore, through phosphorylation of ACS2/ACS6, WRKY33 and ERF1, MPK3/MPK6 are involved in positively regulating both ethylene biosynthesis and signaling, and thus play a critical role in determining the magnitude and kinetics of ethylene signaling outputs in response to pathogen infection.

In addition to regulation of camalexin biosynthesis and ethylene biosynthesis/signaling, MPK3/MPK6 are also involved in regulating the pathogen-responsive IG biosynthesis via ERF6 and MYB51 transcription factors (Xu et al., 2016). Like camalexin, IG is also a Trp-derived indolic antimicrobial metabolite and plays an important role in Arabidopsis immunity (Piasecka et al., 2015). As a substrate of MPK3/MPK6, ERF6 positively regulates the expression of *MYB51*, a

key positive regulator of IG biosynthesis (Gigolashvili et al., 2007; Xu et al., 2016). Interestingly, ethylene signaling is also involved in upregulating *MYB51* expression and thus promoting IG biosynthesis (Clay et al., 2009). Given the ERF6-mediated regulation of *MYB51* expression downstream of MPK3/MPK6 (Xu et al., 2016), we expect that ERF1 is probably involved in regulating *MYB51* expression downstream of ethylene signaling, which needs further study to clarify. In this way, ethylene signaling pathway would also act synergistically with MPK3/MPK6 to induce IG biosynthesis via ERF1/ERF6 and MYB51 transcription factors, meanwhile MPK3/MPK6 and ethylene signaling pathways will act through ERF1/ERF6 and MYB51 to coordinately induce the biosynthesis of Trp-derived indolic antimicrobial metabolites camalexin and IG.

Materials and methods

Plant materials, growth conditions, and treatments

Arabidopsis (*A. thaliana*) ecotypeCol-0 ecotype was used as the wild-type control. All the mutants and transgenic plants used in this study are in the Col-0 background. The knockout mutants *pad3-1* (Glazebrook and Ausubel, 1994), *ein2-1* (Guzman and Ecker, 1990), *coi1-1* (Feys et al., 1994), *ora59-1* (GABI_061A12; Zander et al., 2014), *wrky33-2* (GABI_324B11; Mao et al., 2011), *mpk3-1* (SALK_151594; Ren et al., 2008), and *mpk6-3* (SALK_127507; Liu and Zhang, 2004) were described previously. The double mutant *ein2-1 coi1-1* and the triple mutants *ein2-1 coi1-1 mpk3-1* and *ein2-1 coi1-1 mpk6-3* were generated by genetic crossing, and homozygous lines were used for the experiments. The other mutants used in this study, including *erf1-c1*, *erf1-c2*, *ora59-1 erf96-c1*, *erf1-c1 wrky33-2*, and *erf1-c2 wrky33-2* were generated via CRISPR/Cas9-mediated gene editing, as described below. The conditional double mutant *mpk3 mpk6 pMPK6:MPK6*^{Y144G} was generously provided by Drs Shuqun Zhang and Juan Xu (Xu et al., 2014).

Arabidopsis seedlings were grown on half-strength Murashige and Skoog plates for 7 days at 22°C in a growth chamber with a 12-h light (intensity: 60 μE m^{-2} s^{-1}, from white fluorescent lamps)/12-h dark cycle, then transferred to 6 mL of liquid half-strength Murashige and Skoog medium in 20-mL gas chromatography vials (10 seedlings per vial), and cultured for another 7 days under continuous fluorescent light (intensity: 60 μE m^{-2} s^{-1}, from white fluorescent lamps) to avoid the effect of the light/dark cycle on metabolite biosynthesis and gene expression. Thereafter, the seedlings in gas chromatography vials were inoculated with *B. cinerea* (strain T4) spores (8×10^4 spores mL^{-1}) or *Pst* DC3000 with a final optical density at 600 nm (OD600) of 0.02, or treated with 20-μM ACC, 50-μM MeJA, 10-μM Est, 5-μM Dex, or solvent controls. At indicated time points after treatment, samples of liquid medium and seedlings were collected to analyze metabolite production and gene expression, respectively.

Generation of recombinant plasmids

The coding sequences of *ERF1*, *MPK3*, and *WRKY33*, and the truncated fragments $ERF1_N$ and $ERF1_{DB+C}$ were PCR amplified from Arabidopsis Col-0 cDNA. The S8A, S14A, S22A, 3SA, and 3SD mutations were introduced into $ERF1_N$ or *ERF1* by site-directed mutagenesis. $MPK3^{CA}$ was generated by introduction of D193G and E197A mutations into *MPK3* via site-directed mutagenesis (Berriri et al., 2012). The wild-type, truncated, or mutated version of *ERF1*, *MPK3*, or *WRKY33* were cloned into plant expression vectors, protoplast transfection vectors, or *Escherichia coli* expression vectors as indicated in Supplemental Table S1 to generate the recombinant plasmids used in this study. In addition, the recombinant plasmids *pET28a-6×His-WRKY33-HA*, *pGEX-4T-1-GST-CPK5*, *pHBT-35S:WRKY33-HA*, *pHBT-35S:MKK5*^{DD}*-FLAG*, and *pBI121-35S:4myc-WRKY33* used in this study were generated previously (Zhou et al., 2020).

The effector, reporter, and reference vectors used for the LUC reporter-aided analysis of promoter activity or transactivation activity in Arabidopsis protoplasts were described previously (Li et al., 2015). The reporter constructs $CYP71A13_{pro}$*:LUC* and $PAD3_{pro}$*:LUC* were generated previously for promoter activity assays (Zhou et al., 2020). In this study, *ERF1* and its mutants were cloned into the effector vector and fused to *GAL4DB* to generate the recombinant effector constructs for transactivation assays (Supplemental Table S1). The vectors used for the split-YFP-based BiFC assay were also described previously (Zhou et al., 2014). For BiFC assays in this study, *ERF1*, *ERF7*, *WRKY33*, and *WRKY71* were cloned into the BiFC vectors and fused with the N- or C-terminal half of YFP (Supplemental Table S1). The *35S:NLS-RFP* construct used to visualize the protoplast nuclei was generated previously (Li et al., 2015).

To generate *erf1* and *erf96* mutations via CRISPR/Cas9-mediated gene editing, *ERF1* and *ERF96* gRNA target sequences were designed and synthesized (Supplemental Figure S2; Supplemental Table S2). The *ERF1-* and *ERF96*-editing CRISPR/Cas9 vectors containing a single *ERF1* gRNA and two *ERF96* gRNAs with adjacent targets, respectively (Supplemental Table S1), were generated using the *AtU6-26-gRNA-SK* and *pYAO:hSpCas9* vectors as described previously (Yan et al., 2015). All the primers used for generating the recombinant constructs are listed in Supplemental Table S2.

Generation of transgenic plants and CRISPR/Cas9-induced mutants

Transgenic Arabidopsis plants were generated by *Agrobacterium tumefaciens*-mediated transformation using the floral dip method (Clough and Bent, 1998). For all transgenic plants, 30–50 T1 plants per construct were screened for transgene expression using immunoblotting (IB), and T2 or T3 lines with a single transgene insertion were used for phenotypic characterization. The Arabidopsis transgenic plants used in this study are listed in Supplemental Table S3. To identify *erf1* and *erf96* mutations induced by CRISPR/Cas9-mediated gene editing, the gRNA target regions were PCR amplified from the T1 plants transformed with the

CRISPR/Cas9 vector of *ERF1* or *ERF96*, and then sequenced to screen for homozygous *erf1* or *erf96* mutant in the indicated backgrounds (Supplemental Table S3).

Metabolic analysis

Samples of liquid medium were collected at indicated time points after different treatments. Metabolic analyses were performed using HPLC with fluorescence detection as described previously (Zhou et al., 2020). The camalexin peak was identified by referring to an authentic standard (Sigma-Aldrich, St Louis, MO, USA ; SML1016), and the camalexin concentrations in collected samples were quantified based on the standard curve (peak area versus concentration) of authentic camalexin.

Gene expression analysis

Total RNA extraction, reverse transcription, and qPCR analyses were performed as previously described (He et al., 2019). The transcript of elongation factor 1α (EF1α) was used as a reference. The induction of *CYP71A13*, *PAD3*, *ERF1*, *WRKY33*, *PDF1.2*, and *PR1* expression was calculated as fold induction relative to the basal levels before treatment. The primer pairs used for qPCR are listed in Supplemental Table S2.

Botrytis cinerea resistance assay

Arabidopsis seeds were sown in soil and grown under a 12-h light (intensity: 60 μE m^{-2} s^{-1}, from white fluorescent lamps)/12-h dark cycle in a growth chamber at 22°C and 65% humidity for 4 weeks. To quantify disease resistance, mature rosette leaves were detached and drop-inoculated with 10 μL drops of *B. cinerea* spore suspension (2×10^5 spores mL^{-1}). To investigate the ACC/MeJA-induced disease resistance, rosette leaves were syringe-infiltrated with 20-μM ACC plus 50-μM MeJA at 24 h before leaf detachment for inoculation of *B. cinerea* spore. The *B. cinerea*-inoculated leaves were kept in Petri dishes on wet filter paper. The lesion size was measured at 48 h after inoculation with *B. cinerea*.

Co-IP, BiFC, pull-down, and phosphorylation assays

Arabidopsis protoplast isolation and transfection with the indicated plasmids (Supplemental Table S1) and *A. tumefaciens*-mediated transfection of *N. benthamiana* leaves with the indicated constructs (Supplemental Table S1) were carried out as reported previously (Meng et al., 2016). The transfected protoplasts of *mpk3 mpk6 pMPK6:MPK6*^{Y144G} plants were treated with 5 μM NA-PP1 (MedChemExpress, Monmouth Junction, NJ, USA; HY-13941) for 12 h to block the activation of MPK6^{Y144G}. To investigate the chitin-induced phosphorylation of ERF1, the indicated protoplasts after transfection were treated with 1-μM chitooctaose with eight GlcNAc moieties (IsoSep AB, Stockholm Sweden; 57/12-0010) for 15 min. Total protein extraction from Arabidopsis protoplasts or *N. benthamiana* leaves, protein immunoprecipitation using anti-myc (Abmart, Shanghai, China; M20012) or anti-GFP agarose beads (ChromoTek, Munich, Germany; gta-20), and the IB analyses using indicated antibodies were all performed as previously described (Meng et al., 2016). The BiFC assays in Arabidopsis protoplasts transfected with the indicated plasmids (Supplemental Table S1) were also performed as previously described (Zhou et al., 2014).

Prokaryotic expression and purification of the 6 × His-, GST-, and MBP-fused recombinant proteins and GST pull-down assays using glutathione agarose beads were carried out as previously described (Zhou et al., 2020). In vitro phosphorylation reactions with or without addition of [γ-^{32}P]ATP were also performed as previously described (Zhou et al., 2020), and the phosphorylation of recombinant proteins was analyzed by autoradiography, or by IB with Phostag-Biotin (APExBIO, Houston, TX, USA; F4001) or anti-pThr antibody (Cell Signaling, Danvers, MA, USA; 9381) after protein separation by the sodium dodecyl sulphate-polyacrylamide gel electrophoresis (SDS-PAGE).

EMSA and ChIP-qPCR analysis

The GCC box-containing oligonucleotide probes as shown in Figure 4D were synthesized and labeled with biotin at the 5′-end (Sangon). Gel mobility shift assays were performed using the freshly prepared MBP-ERF1-HA protein and the LightShift Chemiluminescent EMSA Kit (ThermoFisher Scientific, Waltham, MA, USA; 20148) as previously described (Zhou et al., 2020). Two-week-old *35S:4myc-ERF1* transgenic seedlings were used for ChIP-qPCR analysis. Chromatin isolation and immunoprecipitation were carried out as previously described (Zhou et al., 2020). The immunoprecipitated and input DNA samples were analyzed by qPCR using primers specific for the GCC box-containing regions of *CYP71A13* and *PAD3* promoters. The ChIP-qPCR results are presented as percentages of the input DNA.

Analysis of promoter activity and transactivation activity

Arabidopsis protoplasts were co-transfected with the indicated reporter and effector constructs. The reference construct *UBQ10$_{pro}$:GUS* was included in all transfections and served as an internal transfection control. Analyses of the LUC and GUS activities in transfected protoplasts were performed as previously described (Zhou et al., 2020). The promoter and transactivation activities were calculated as the ratio of LUC activity to GUS activity, and the data are shown as relative fold increases over the control.

Statistical analyses

At least three independent repetitions were performed for the experiments in this study. Results from one of the independent repeats that gave similar results were shown. Student's *t* test was used to determine whether the difference between the two groups of data is statistically significant. Asterisks above the columns indicate differences that are statistically significant ($P < 0.05$). When more than two groups of data at a specific time point or from a specific treatment are compared, one-way ANOVA with Tukey's post hoc test was performed ($P < 0.05$). Different letters

above the data points are used to indicate differences that are statistically significant.

Accession numbers

Sequence data from this article can be found in the Arabidopsis Genome Initiative or GenBank/EMBL databases under the following accession numbers: *EIN2* (AT5G03280), *COI1* (AT2G39940), *ERF1* (AT3G23240), *ORA59* (AT1G06160), *ERF96* (AT5G43410), *CYP71A13* (AT2G30770), *PAD3* (AT3G26830), *WRKY33* (AT2G38470), *MPK3* (AT3G45640), *MPK6* (AT2G43790), *MKK5* (AT3G21220), *CPK5* (AT4G35310), *PDF1.2* (AT5G44420), *PR1* (AT2G14610), and *EF1α* (AT5G60390).

Supplemental data

The following materials are available in the online version of this article.

Supplemental Figure S1. Cotreatment of Arabidopsis seedlings with ACC- and MeJA-induced camalexin biosynthesis.

Supplemental Figure S2. Generation of the *erf1-c1*, *erf1-c2*, *erf1-c1 wrky33-2*, *erf1-c2 wrky33-2*, and *ora59-1 erf96-c1* mutants using CRISPR/Cas9 system.

Supplemental Figure S3. *ORA59* and *ERF96* are not involved in regulating *B. cinerea*-induced camalexin biosynthesis.

Supplemental Figure S4. Overexpression of *ERF1* led to the WRKY33-dependent activation of defense genes *PDF1.2* and *PR1*.

Supplemental Figure S5. The *erf1-c1* mutants showed defects in both the basal and the ACC/MeJA-induced resistance to *B. cinerea*.

Supplemental Figure S6. Overexpression of *ERF1* resulted in the WRKY33-dependent enhancement of resistance to *B. cinerea*.

Supplemental Figure S7. Chemically induced expression of *ERF1* but not *WRKY33* was able to induce camalexin biosynthesis in transgenic Arabidopsis plants.

Supplemental Figure S8. WRKY33 is required for the ERF1-mediated potentiation of camalexin biosynthetic gene activation in response to *B. cinerea* infection.

Supplemental Figure S9. WRKY33 is required for ERF1-mediated activation of *CYP71A13* and *PAD3* promoters in Arabidopsis protoplasts.

Supplemental Figure S10. The *erf1-c1 wrky33-2* and *wrky33-2* mutants exhibited comparable levels of defects in *B. cinerea*-induced camalexin biosynthetic gene activation.

Supplemental Figure S11. ERF1 and WRKY33 additively activate *CYP71A13* and *PAD3* promoters in Arabidopsis protoplasts.

Supplemental Figure S12. *ERF1* and *WRKY33* do not regulate the expression of each other in response to *B. cinerea* infection.

Supplemental Figure S13. *ERF1* and *WRKY33* are both required for the induction of camalexin biosynthesis in Arabidopsis upon infection by *Pst* DC3000.

Supplemental Figure S14. The basal expression level of *WRKY33* is much higher than that of *ERF1*.

Supplemental Figure S15. CPK5 cannot phosphorylate ERF1 in vitro.

Supplemental Table S1. Recombinant plasmids generated in this study.

Supplemental Table S2. Primers used in this study.

Supplemental Table S3. Transgenic Arabidopsis plants generated in this study.

Supplemental Data Set 1. Results of ANOVAs and *t* tests for the data presented in each figure.

Acknowledgments

We thank Drs. Shuqun Zhang and Juan Xu for providing the *mpk3 mpk6 pMPK6:MPK6*^{Y144G} transgenic seeds, Drs. Ping He, Libo Shan, and Bo Li for providing plant or protoplast transformation vectors, Dr. Qi Xie for providing CRISPR/Cas9 vectors, Drs. Yiwen Deng and Zuhua He for assistance in phosphorylation assays, and Dr. Jiming Gong and the ABRC for providing Arabidopsis mutant seeds.

Funding

This work was supported by the National Natural Science Foundation of China (Grant 31800215 to J.Zho. and Grant 31970282 to X.M.) and the Shanghai Rising-Star Program (Grant 20QA1407600 to J.Zho.).

Conflict of interest statement. None declared.

References

Aerts N, Pereira Mendes M, Van Wees SCM (2021) Multiple levels of crosstalk in hormone networks regulating plant defense. Plant J **105**: 489–504

Bednarek P, Pislewska-Bednarek M, Svatos A, Schneider B, Doubsky J, Mansurova M, Humphry M, Consonni C, Panstruga R, Sanchez-Vallet A, et al. (2009) A glucosinolate metabolism pathway in living plant cells mediates broad-spectrum antifungal defense. Science **323**: 101–106

Berriri S, Garcia AV, Frei dit Frey N, Rozhon W, Pateyron S, Leonhardt N, Montillet JL, Leung J, Hirt H, Colcombet J (2012) Constitutively active mitogen-activated protein kinase versions reveal functions of Arabidopsis MPK4 in pathogen defense signaling. Plant Cell **24**: 4281–4293

Bigeard J, Colcombet J, Hirt H (2015) Signaling mechanisms in pattern-triggered immunity (PTI). Mol Plant **8**: 521–539

Binder BM (2020) Ethylene signaling in plants. J Biol Chem **295**: 7710–7725

Birkenbihl RP, Kracher B, Roccaro M, Somssich IE (2017) Induced genome-wide binding of three Arabidopsis WRKY transcription factors during early MAMP-triggered immunity. Plant Cell **29**: 20–38

Bishop AC, Ubersax JA, Petsch DT, Matheos DP, Gray NS, Blethrow J, Shimizu E, Tsien JZ, Schultz PG, Rose MD, et al. (2000) A chemical switch for inhibitor-sensitive alleles of any protein kinase. Nature **407**: 395–401

Bottcher C, Westphal L, Schmotz C, Prade E, Scheel D, Glawischnig E (2009) The multifunctional enzyme CYP71B15 (PHYTOALEXIN DEFICIENT3) converts cysteine-indole-3-acetonitrile to camalexin in the indole-3-acetonitrile metabolic network of *Arabidopsis thaliana*. Plant Cell **21**: 1830–1845

Burger M, Chory J (2019) Stressed out about hormones: how plants orchestrate immunity. Cell Host Microbe **26**: 163–172

Catinot J, Huang JB, Huang PY, Tseng MY, Chen YL, Gu SY, Lo WS, Wang LC, Chen YR, Zimmerli L (2015) ETHYLENE RESPONSE FACTOR 96 positively regulates Arabidopsis resistance to necrotrophic pathogens by direct binding to GCC elements of jasmonate - and ethylene-responsive defence genes. Plant Cell Environ **38**: 2721–2734

Clay NK, Adio AM, Denoux C, Jander G, Ausubel FM (2009) Glucosinolate metabolites required for an Arabidopsis innate immune response. Science **323**: 95–101

Clough SJ, Bent AF (1998) Floral dip: a simplified method for Agrobacterium-mediated transformation of *Arabidopsis thaliana*. Plant J **16**: 735–743

Cui H, Tsuda K, Parker JE (2015) Effector-triggered immunity: from pathogen perception to robust defense. Annu Rev Plant Biol **66**: 487–511

DeFalco TA, Zipfel C (2021) Molecular mechanisms of early plant pattern-triggered immune signaling. Mol Cell **81**: 3449–3467

Feys B, Benedetti CE, Penfold CN, Turner JG (1994) Arabidopsis mutants selected for resistance to the phytotoxin coronatine are male sterile, insensitive to methyl jasmonate, and resistant to a bacterial pathogen. Plant Cell **6**: 751–759

Frerigmann H, Glawischnig E, Gigolashvili T (2015) The role of MYB34, MYB51 and MYB122 in the regulation of camalexin biosynthesis in *Arabidopsis thaliana*. Front Plant Sci **6**: 654

Geu-Flores F, Moldrup ME, Bottcher C, Olsen CE, Scheel D, Halkier BA (2011) Cytosolic gamma-glutamyl peptidases process glutathione conjugates in the biosynthesis of glucosinolates and camalexin in Arabidopsis. Plant Cell **23**: 2456–2469

Gigolashvili T, Berger B, Mock HP, Muller C, Weisshaar B, Flugge UI (2007) The transcription factor HIG1/MYB51 regulates indolic glucosinolate biosynthesis in *Arabidopsis thaliana*. Plant J **50**: 886–901

Glazebrook J, Ausubel FM (1994) Isolation of phytoalexin-deficient mutants of *Arabidopsis thaliana* and characterization of their interactions with bacterial pathogens. Proc Natl Acad Sci USA **91**: 8955–8959

Guzman P, Ecker JR (1990) Exploiting the triple response of Arabidopsis to identify ethylene-related mutants. Plant Cell **2**: 513–523

Han L, Li GJ, Yang KY, Mao G, Wang R, Liu Y, Zhang S (2010) Mitogen-activated protein kinase 3 and 6 regulate *Botrytis cinerea*-induced ethylene production in Arabidopsis. Plant J **64**: 114–127

He Y, Xu J, Wang X, He X, Wang Y, Zhou J, Zhang S, Meng X (2019) The Arabidopsis pleiotropic drug resistance transporters PEN3 and PDR12 mediate camalexin secretion for resistance to *Botrytis cinerea*. Plant Cell **31**: 2206–2222

Hiruma K, Fukunaga S, Bednarek P, Pislewska-Bednarek M, Watanabe S, Narusaka Y, Shirasu K, Takano Y (2013) Glutathione and tryptophan metabolism are required for Arabidopsis immunity during the hypersensitive response to hemibiotrophs. Proc Natl Acad Sci USA **110**: 9589–9594

Howe GA, Major IT, Koo AJ (2018) Modularity in jasmonate signaling for multistress resilience. Annu Rev Plant Biol **69**: 387–415

Huang PY, Catinot J, Zimmerli L (2016) Ethylene response factors in Arabidopsis immunity. J Exp Bot **67**: 1231–1241

Jones JD, Dangl JL (2006) The plant immune system. Nature **444**: 323–329

Ju C, Chang C (2015) Mechanistic insights in ethylene perception and signal transduction. Plant Physiol **169**: 85–95

Li B, Jiang S, Yu X, Cheng C, Chen S, Cheng Y, Yuan JS, Jiang D, He P, Shan L (2015) Phosphorylation of trihelix transcriptional repressor ASR3 by MAP KINASE4 negatively regulates Arabidopsis immunity. Plant Cell **27**: 839–856

Li G, Meng X, Wang R, Mao G, Han L, Liu Y, Zhang S (2012) Dual-level regulation of ACC synthase activity by MPK3/MPK6 cascade and its downstream WRKY transcription factor during ethylene induction in Arabidopsis. PLoS Genet **8**: e1002767

Li Y, Liu K, Tong G, Xi C, Liu J, Zhao H, Wang Y, Ren D, Han S (2022) MPK3/MPK6-mediated phosphorylation of ERF72 positively regulates resistance to *Botrytis cinerea* through directly and indirectly activating the transcription of camalexin biosynthesis enzymes. J Exp Bot **73**: 413–428

Liu Y, Zhang S (2004) Phosphorylation of 1-aminocyclopropane-1--carboxylic acid synthase by MPK6, a stress-responsive mitogen-activated protein kinase, induces ethylene biosynthesis in Arabidopsis. Plant Cell **16**: 3386–3399

Lorenzo O, Piqueras R, Sanchez-Serrano JJ, Solano R (2003) ETHYLENE RESPONSE FACTOR1 integrates signals from ethylene and jasmonate pathways in plant defense. Plant Cell **15**: 165–178

Mao G, Meng X, Liu Y, Zheng Z, Chen Z, Zhang S (2011) Phosphorylation of a WRKY transcription factor by two pathogen-responsive MAPKs drives phytoalexin biosynthesis in Arabidopsis. Plant Cell **23**: 1639–1653

Meng X, Zhang S (2013) MAPK cascades in plant disease resistance signaling. Annu Rev Phytopathol **51**: 245–266

Meng X, Zhou J, Tang J, Li B, de Oliveira MVV, Chai J, He P, Shan L (2016) Ligand-induced receptor-like kinase complex regulates floral organ abscission in Arabidopsis. Cell Rep **14**: 1330–1338

Nafisi M, Goregaoker S, Botanga CJ, Glawischnig E, Olsen CE, Halkier BA, Glazebrook J (2007) Arabidopsis cytochrome P450 monooxygenase 71A13 catalyzes the conversion of indole-3-acetaldoxime in camalexin synthesis. Plant Cell **19**: 2039–2052

Peng Y, Yang J, Li X, Zhang Y (2021) Salicylic acid: biosynthesis and signaling. Annu Rev Plant Biol **72**: 761–791

Piasecka A, Jedrzejczak-Rey N, Bednarek P (2015) Secondary metabolites in plant innate immunity: conserved function of divergent chemicals. New Phytol **206**: 948–964

Pre M, Atallah M, Champion A, De Vos M, Pieterse CM, Memelink J (2008) The AP2/ERF domain transcription factor ORA59 integrates jasmonic acid and ethylene signals in plant defense. Plant Physiol **147**: 1347–1357

Qi J, Wang J, Gong Z, Zhou JM (2017) Apoplastic ROS signaling in plant immunity. Curr Opin Plant Biol **38**: 92–100

Qiu J, Fiil BK, Petersen K, Nielsen HB, Botanga CJ, Thorgrimsen S, Palma K, Suarez-Rodriguez MC, Sandbech-Clausen S, Lichota J, et al. (2008) Arabidopsis MAP kinase 4 regulates gene expression through transcription factor release in the nucleus. EMBO J **27**: 2214–2221

Ren D, Liu Y, Yang KY, Han L, Mao G, Glazebrook J, Zhang S (2008) A fungal-responsive MAPK cascade regulates phytoalexin biosynthesis in Arabidopsis. Proc Natl Acad Sci USA **105**: 5638–5643

Saga H, Ogawa T, Kai K, Suzuki H, Ogata Y, Sakurai N, Shibata D, Ohta D (2012) Identification and characterization of ANAC042, a transcription factor family gene involved in the regulation of camalexin biosynthesis in Arabidopsis. Mol Plant Microbe Interact **25**: 684–696

Schlaeppi K, Abou-Mansour E, Buchala A, Mauch F (2010) Disease resistance of Arabidopsis to Phytophthora brassicae is established by the sequential action of indole glucosinolates and camalexin. Plant J **62**: 840–851

Schuhegger R, Nafisi M, Mansourova M, Petersen BL, Olsen CE, Svatos A, Halkier BA, Glawischnig E (2006) CYP71B15 (PAD3) catalyzes the final step in camalexin biosynthesis. Plant Physiol **141**: 1248–1254

Seybold H, Trempel F, Ranf S, Scheel D, Romeis T, Lee J (2014) Ca2 + signalling in plant immune response: from pattern recognition receptors to Ca2 + decoding mechanisms. New Phytol **204**: 782–790

Solano R, Stepanova A, Chao Q, Ecker JR (1998) Nuclear events in ethylene signaling: a transcriptional cascade mediated by

ETHYLENE-INSENSITIVE3 and ETHYLENE-RESPONSE-FACTOR1. Genes Dev **12**: 3703–3714

Sonderby IE, Geu-Flores F, Halkier BA (2010) Biosynthesis of glucosinolates – gene discovery and beyond. Trends Plant Sci **15**: 283–290

Song S, Qi T, Wasternack C, Xie D (2014) Jasmonate signaling and crosstalk with gibberellin and ethylene. Curr Opin Plant Biol **21**: 112–119

Stotz HU, Sawada Y, Shimada Y, Hirai MY, Sasaki E, Krischke M, Brown PD, Saito K, Kamiya Y (2011) Role of camalexin, indole glucosinolates, and side chain modification of glucosinolate-derived isothiocyanates in defense of Arabidopsis against Sclerotinia sclerotiorum. Plant J **67**: 81–93

Su T, Xu J, Li Y, Lei L, Zhao L, Yang H, Feng J, Liu G, Ren D (2011) Glutathione-indole-3-acetonitrile is required for camalexin biosynthesis in *Arabidopsis thaliana*. Plant Cell **23**: 364–380

Thomma BP, Nelissen I, Eggermont K, Broekaert WF (1999) Deficiency in phytoalexin production causes enhanced susceptibility of *Arabidopsis thaliana* to the fungus Alternaria brassicicola. Plant J **19**: 163–171

Tsuji J, Jackson EP, Gage DA, Hammerschmidt R, Somerville SC (1992) Phytoalexin accumulation in *Arabidopsis thaliana* during the hypersensitive reaction to *Pseudomonas syringae* pv syringae. Plant Physiol **98**: 1304–1309

Wang W, Feng B, Zhou JM, Tang D (2020) Plant immune signaling: advancing on two frontiers. J Integr Plant Biol **62**: 2–24

Xu J, Meng J, Meng X, Zhao Y, Liu J, Sun T, Liu Y, Wang Q, Zhang S (2016) Pathogen-responsive MPK3 and MPK6 reprogram the biosynthesis of indole glucosinolates and their derivatives in Arabidopsis immunity. Plant Cell **28**: 1144–1162

Xu J, Xie J, Yan C, Zou X, Ren D, Zhang S (2014) A chemical genetic approach demonstrates that MPK3/MPK6 activation and NADPH oxidase-mediated oxidative burst are two independent signaling events in plant immunity. Plant J **77**: 222–234

Yan L, Wei S, Wu Y, Hu R, Li H, Yang W, Xie Q (2015) High-efficiency genome editing in Arabidopsis using YAO promoter-driven CRISPR/Cas9 system. Mol Plant **8**: 1820–1823

Yang L, Zhang Y, Guan R, Li S, Xu X, Zhang S, Xu J (2020) Co-regulation of indole glucosinolates and camalexin biosynthesis by CPK5/CPK6 and MPK3/MPK6 signaling pathways. J Integr Plant Biol **62**: 1780–1796

Yuan M, Ngou BPM, Ding P, Xin XF (2021) PTI-ETI crosstalk: an integrative view of plant immunity. Curr Opin Plant Biol **62**: 102030

Zander M, Thurow C, Gatz C (2014) TGA transcription factors activate the salicylic acid-suppressible branch of the ethylene-induced defense program by regulating ORA59 expression. Plant Physiol **165**: 1671–1683

Zhang L, Zhang F, Melotto M, Yao J, He SY (2017a) Jasmonate signaling and manipulation by pathogens and insects. J Exp Bot **68**: 1371–1385

Zhang W, Corwin JA, Copeland D, Feusier J, Eshbaugh R, Chen F, Atwell S, Kliebenstein DJ (2017b) Plastic transcriptomes stabilize immunity to pathogen diversity: the jasmonic acid and salicylic acid networks within the Arabidopsis/Botrytis pathosystem. Plant Cell **29**: 2727–2752

Zhao K, Kong D, Jin B, Smolke CD, Rhee SY (2021) A novel bivalent chromatin associates with rapid induction of camalexin biosynthesis genes in response to a pathogen signal in Arabidopsis. Elife **10**: e69508

Zhao Y, Hull AK, Gupta NR, Goss KA, Alonso J, Ecker JR, Normanly J, Chory J, Celenza JL (2002) Trp-dependent auxin biosynthesis in Arabidopsis: involvement of cytochrome P450s CYP79B2 and CYP79B3. Genes Dev **16**: 3100–3112

Zhou J, Wang X, He Y, Sang T, Wang P, Dai S, Zhang S, Meng X (2020) Differential phosphorylation of the transcription factor WRKY33 by the protein kinases CPK5/CPK6 and MPK3/MPK6 cooperatively regulates camalexin biosynthesis in Arabidopsis. Plant Cell **32**: 2621–2638

Zhou J, Wu S, Chen X, Liu C, Sheen J, Shan L, He P (2014) The *Pseudomonas syringae* effector HopF2 suppresses Arabidopsis immunity by targeting BAK1. Plant J **77**: 235–245

Zhou JM, Zhang Y (2020) Plant immunity: danger perception and signaling. Cell **181**: 978–989

Zhou N, Tootle TL, Glazebrook J (1999) Arabidopsis PAD3, a gene required for camalexin biosynthesis, encodes a putative cytochrome P450 monooxygenase. Plant Cell **11**: 2419–2428

Zhu QG, Gong ZY, Huang J, Grierson D, Chen KS, Yin XR (2019) High-CO2/hypoxia-responsive transcription factors DkERF24 and DkWRKY1 interact and activate DkPDC2 promoter. Plant Physiol **180**: 621–633

Zhu Z, An F, Feng Y, Li P, Xue LAM, Jiang Z, Kim JM, To TK, Li W, Zhang X, et al. (2011) Derepression of ethylene-stabilized transcription factors (EIN3/EIL1) mediates jasmonate and ethylene signaling synergy in Arabidopsis. Proc Natl Acad Sci USA **108**: 12539–12544